AN INVESTIGATION OF THE PRINCIPLES AND PRACTICES OF SEISMIC ISOLATION IN BRIDGE STRUCTURES

by

Evan M. Lapointe

Bachelor of Engineering in Civil Engineering
The Cooper Union for the Advancement of Science and Art, 2003

Submitted to the Department of Civil and Environmental Engineering
In Partial Fulfillment of the Requirements for the Degree of

Master of Engineering
In Civil and Environmental Engineering

at the

MASSACHUSETTS INSTITUTE OF TECHNOLOGY

June 2004

Signature of Author_____
Department of Civil and Environmental Engineering
May 7, 2004

Certified by_____
Jerome J. Connor
Professor of Civil and Environmental Engineering
Thesis Supervisor

Accepted by _____
Heidi Nepf
Chairman, Departmental Committee on Graduate Studies

AN INVESTIGATION OF THE PRINCIPLES AND PRACTICES OF SEISMIC ISOLATION IN BRIDGE STRUCTURES

by

Evan M. Lapointe

Submitted to the Department of Civil and Environmental Engineering
On May 7, 2004
In Partial Fulfillment of the Requirements for the Degree of Master of Engineering
In Civil and Environmental Engineering

ABSTRACT

Within the past decade, seismic isolation systems have gained rapid popularity in the earthquake resistant design of bridge structures. This popularity has come in response to the inadequacy of earlier seismic design and retrofit methodologies. The mechanical shortcomings and subsequent failure mechanisms associated with the early elastic seismic design philosophy are first presented, followed by a study of the applicability of seismic isolation systems in bridge structures. This investigation includes a discussion of the susceptibility of simple span bridges to seismic failure, an overview of the behavior of base isolated structures, a detailed description of isolation system components, an explanation of the mechanics of elastometric isolation bearings, and a presentation of the linear theory of seismic isolation.

The qualitative investigation of seismic isolation systems is supplemented by a quantitative nonlinear time-history analysis that illustrates the response of a simple span bridge to seismic excitation. The analysis examines the effects of the varying stiffness of a lead-rubber elastometric bearing upon structural response when subjected to the 1940 El Centro earthquake. The results confirm the expected behavior of isolated structures and emphasize the need for site-specific studies in the design of effective seismic isolation systems for bridge structures.

Thesis Supervisor: Jerome J. Connor
Title: Professor of Civil and Environmental Engineering

ACKNOWLEDGEMENTS

This thesis would not have been possible without the support and inspiration of so many people that have contributed to my personal and intellectual growth over the last several years.

First and foremost, I would like to thank Mr. Peter Cooper, a man who believed that education should be as free as air and water. Without the unique vision and generous philanthropy of Mr. Cooper, I certainly would never have found myself at MIT. Mr. Cooper, I hope I've made you proud.

I would also like to thank Professor Jerome Connor, whose incredible energy, devotion to his students, and knowledge of structural engineering is nothing short of inspirational.

I'd like to thank my family for providing me with financial and emotional support while I've been away at school. Mom and Dad, thank you for helping me achieve my dreams, and Neil, thank you for always giving me somebody to look up to and for inspiring me to reach higher.

I certainly can't forget to thank the friends I've made, both at The Cooper Union and at MIT, who have given me support and memories that won't be forgotten. I'd like to thank my numerous roommates on Baxter Street for providing me with more than enough amusing memories to make it through MIT. I'd like to thank Cody Fleming for his friendship over the past year, and for helping me through innumerable problem sets. I'd like to thank the usual crowd in the M.Eng. bullpen, where countless hours were spent, and where I could always count on laughs to make it through the worst days. I'd also like to thank John Broderick and Matt Salmonsen for forcing me to close my books and live a little and for showing me the world outside of engineering.

And finally, I'd like to thank Brenda Holian for her constant encouragement, patience, and love, even when it wasn't deserved.

TABLE OF CONTENTS

LIST OF FIGURES

LIST OF TABLES

CHAPTER 1: INTRODUCTION TO SEISMIC ISOLATION SYSTEMS

1.1 Overview

Bridges and transportation viaducts are ubiquitous in today's built environment, carrying highways through cities and countries and serving as the transportation lifeline of modern society. Without bridges, transportation would cease, commerce would subsequently halt, and the economy of modern society would cease to exist. Thus, the importance of bridge structures cannot be underestimated, and bridges must be designed to adequately withstand the forces of catastrophic events, namely devastating earthquakes. The vitality of transportation networks must be ensured and the safety of the users of transportation infrastructure must be guaranteed.

The necessity to construct and rehabilitate bridge structures to withstand seismic forces in earthquake-prone regions is more than a mere philosophy. The fairly recent 1989 Loma Prieta earthquake and 1994 Northridge earthquake in California in addition to the 1995 Kobe earthquake in Japan have demonstrated the need for further research and thought in seismic resistant design. These earthquakes, which occurred in densely populated areas, caused either collapse or severe damage to bridges that were specifically designed to resist earthquakes of a greater intensity than the actual applied seismic excitation [1].

1.2 Earthquake Design Background

Part of the problem involving the seismic inadequacy of bridge structures stems from the seismic design methodology practiced prior to 1970. Near the end of the millennium, about 60% of all highway bridges in the United States, approximately 350,000, were constructed prior to 1970 [2]. During this time period, insufficient consideration was given to seismic forces, and bridges designed and constructed during this era have proven wholly inadequate in the wake of seismic events. Initial seismic deign methodologies emphasized an elastic approach, where bridge structures were designed to undergo elastic deformations when subjected to seismic forces. The structural stiffness resulting from the elastic design methodology resulted in low levels of ductility and subsequently small amounts of dissipated energy. Stiffness also tends to

amplify ground motions, resulting in increased structural acceleration. Furthermore, the increased stiffness results in greater structural mass that increases internal shear forces within the structure due to the aforementioned amplified accelerations. The consequences of the initial elastic design approach resulted in severely underestimated seismic deflections in addition to underestimated and inaccurate moment patterns in bridge structures [1]. Consequences resulting from elastic design included deck seats and corbels of insufficient length and inadequate design of major structural components of the bridge, particularly supporting columns. These design inadequacies resulted in the collapse and severe damage of bridge structures and the subsequent loss of life.

It is now known that structural ductility is crucial in dissipating seismic energy within structures. An inelastic seismic design philosophy has been adopted that incorporates the formation of plastic hinges, allowing inelastic structural deformations to dissipate energy. Thus, potentially devastating seismic forces are reduced. However, the critical flaw of this methodology is the necessity for the structure to experience damage. While the damage is not as severe as in the case of elastic seismic design, it still results in cost to taxpayers and temporary bridge closure to facilitate repair.

1.3 Introduction to Seismic Isolation

Ideally, a structure should remain elastic during seismic excitation to avoid damage and should also retain the ability to undergo large deformations to facilitate energy dissipation. These demands seem paradoxical with the application of traditional structural materials, but the two extremes can be accomplished via the increasingly popular philosophy of seismic isolation.

Seismic isolation, or base isolation, has gained design popularity within the last quarter century and is applicable to bridge structures as well as building structures. Seismic isolation allows for a decrease in seismic demand via relative structural displacement rather than an increase in structural stiffness. As mentioned above, increased structural stiffness increases strength but tends to attract greater seismic forces through amplified accelerations and increased structural mass. Through the application of seismic isolation in bridges, not only can appreciable relative deflections be tolerated, but major structural components can also remain in the elastic deformation range when

subjected to earthquake loads. Deflections are confined to the isolated superstructure level, and lateral forces in supporting columns and abutments are significantly reduced.

The basic premise of seismic isolation is the decoupling of the isolated portion of the structure from horizontal lateral earthquake motion. The decoupling is accomplished through the implementation of base isolation bearings with very small lateral stiffness in comparison to the lateral stiffness of the structure. The decoupling results in a shift of the fundamental period of the isolated structure out of the range of the predominant period of seismic excitation. This period shift significantly reduces the effective magnitude of applied seismic loads.

The first dynamic mode involves only the deformation of the isolated structure rather than the deformation of the entire structure for the case of a non-isolated system. In the case of bridges, if only the superstructure is isolated, then only the superstructure will experience deformation in the first dynamic mode, assuming an extremely rigid deck structure in comparison to the substructure. Furthermore, energy from ground motion has little effect upon the excitation of higher modes. Higher dynamic modes have a low participation factor in the response of the structure because these modes are orthogonal to both the first mode and to ground motion [3]. Hence, in the analysis of seismically isolated structures, generally only the first dynamic mode is of interest.

1.4 Applicability to Bridge Structures

Seismic isolation is readily applicable to bridge structures, especially simple span highway bridges, due to both inherent structural inadequacies and adaptive structural characteristics. Structural inadequacies of these simple span bridge types include two intrinsic flaws that make them particularly susceptible to earthquake damage and that warrant the need for increased seismic resistance. These two flaws are the lack of structural redundancy and the inbuilt natural frequency. Since nearly all simple span bridges are purely functional, they lack the redundant structural systems inherent in building structures that prevent complete collapse. Furthermore, simple span bridges tend to have natural frequencies that coincide with the dominant excitation frequency of most earthquakes.

In terms of adaptive structural characteristics, simple span bridges possess geometries and structural systems that lend themselves to the implementation of base isolation systems. First, the majority of the mass in bridge structures is concentrated at the deck level, which is generally the isolated level. Second, most simple span bridge superstructures are already constructed on expansion bearings, thus base isolation bearings can simply replace the expansion bearings without imposing additional structural members. Third, in the case of an extreme seismic event, any structural damage theoretically is confined only to isolation bearings, and these bearings can be easily inspected and replaced. Finally, installation of base isolation systems in existing bridge structures can be accomplished while the bridge is partially open to traffic.

CHAPTER 2: PAST PROBLEMS AND FAILURES IN BRIDGE STRUCTURES

2.1 Introduction

To fully comprehend the relevance and benefits of seismic isolation systems, the nature of seismic damage to bridge structures and the various failure mechanisms are first examined. Widespread seismic damage has occurred to bridge structures during past earthquakes, namely simply supported highway bridges, and many spans have suffered complete failure. The destructive power of earthquakes is shown below in Figure 2-1, where a simply supported highway overpass was completely destroyed in the 1971 San Fernando earthquake [4]. Seismic damage and failure in highway bridges can be categorized according to the type of failure mechanism that affects major components of the bridge, including span displacement, abutment slumping, column failure, cap beam failure, joint failure, footing failure, and failure of superstructure components. Since displacement and column failures seem to cause the most significant and costly damage in bridges, and since seismic isolation systems can remedy displacement failures and readily reduce internal column forces, the mechanisms causing these failures will be investigated in detail.

Figure 2-1: Severe seismic damage to highway bridge spans.

While significant damage has occurred to bridges of both steel and reinforced concrete construction, failure mechanisms in reinforced concrete members are examined in greater detail in this chapter for two primary reasons. First, damage occurring to supporting columns often results in the complete failure of the bridge span, and supporting columns are more often constructed of reinforced concrete. Second, steel members tend to exhibit greater levels of ductility and can therefore dissipate energy when subjected to seismic excitation, avoiding total failure.

2.2 Displacement Failures

Displacements are a major cause of highway bridge span damage and failure during earthquakes. Displacement failure due to seismic excitation is the result of concrete bridge design using elastic theory. The underestimated lateral forces and overestimated gross-section stiffness resulted in the inadequate design of superstructure seats and lateral clearance between adjacent structures [1]. Two damaging displacement mechanisms of interest that are prevalent in reinforced concrete bridges are unseating and pounding. Excessive displacements in the longitudinal direction can result in bridge failure via the unseating of the superstructure, while displacements in the transverse direction can result in pounding damage through cyclic contact with an adjacent structure.

2.2.1 Unseating Failures

Unseating failure is particularly problematic for simply supported highway bridges when earthquake excitation occurs in the longitudinal direction. If seats or corbels located at the abutments or on the piers do not possess sufficient length in the longitudinal direction, then the entire superstructure span can become unseated, resulting in sudden bridge collapse. This failure mechanism can be enhanced for either tall pier columns or for adjacent pier frames of unequal height. In the case of tall piers, column rotation about the base enhances displacements at the location of maximum height of the superstructure. Adjacent pier frames of varying heights have different fundamental frequencies, and thus displacements are increased if the frames respond out of phase with

respect to each other when subjected to seismic excitation. An example of unseating failure that occurred during the 1999 Chi-Chi earthquake in Taiwan is shown below in Figure 2-2 [5].

Figure 2-2: Unseating failure.

2.2.2 Pounding Damage

Pounding of bridge structures due to inadequate displacement considerations can also result in severe bridge damage. If a small clearance envelope exists between the bridge and adjacent structures, then damage can occur through cyclic pounding as the earthquake occurs in the transverse direction, creating shear forces and imposing brittle failure. This damage can be amplified if the adjacent structure is of a different height or stiffness. The different fundamental frequency of the adjacent structure can result in out of phase motion with the bridge, amplifying shear forces and corresponding pounding damage.

2.3 Column Failures

The study of column failure during seismic activity is significant because collapse of a supporting column within a pier group will likely result in the failure of the entire bridge structure. The devastating effects of this failure mechanism are shown below in Figure 2-3, which depicts the complete destruction of an overpass in California due to column failure during the 1994 Northridge earthquake [2]. The two primary failure

mechanisms that occur in columns are flexural and inadequate ductility failure and shear failure. The mechanics of these failures are discussed below.

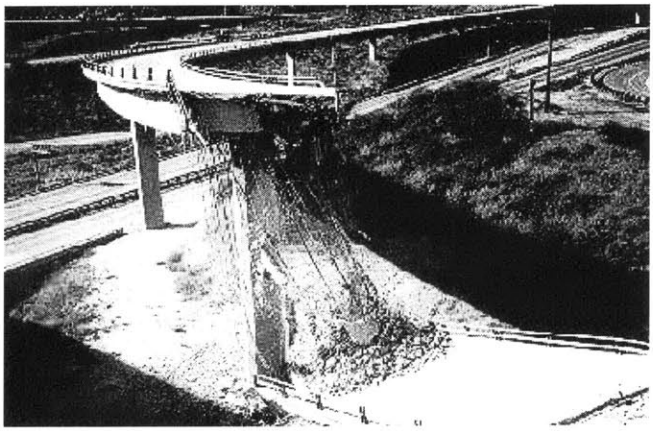

Figure 2-3: Span collapse resulting from complete column failure.

2.3.1 Column Flexural Failure

Flexural failure within supporting columns tends to result from the obsolete elastic design philosophy or from deficient reinforcement design and installation. Common flexural deficiencies include inadequate strength, undependable strength, inadequate ductility, and premature termination of reinforcement. While these failure deficiencies will be discussed separately, failure in columns generally results from a combination of several of the named mechanisms.

2.3.1.1 Inadequate Column Flexural Strength

The first major flexural deficiency in supporting columns and piers that will be examined is inadequate flexural strength. Before an inelastic design methodology was utilized that considered plastic deformation and subsequent energy dissipation, equivalent lateral seismic forces were underestimated, and the corresponding elastic design was insufficient. The discrepancy between actual column strength and the elastic design level is illustrated in the column axial force-bending moment interaction diagram shown in Figure 2-4 [1]. The difference between the elastic design curve and strength design curve in this diagram seems significant, but actual elastic design levels for columns were enhanced in practice due to the conservative nature of engineering design.

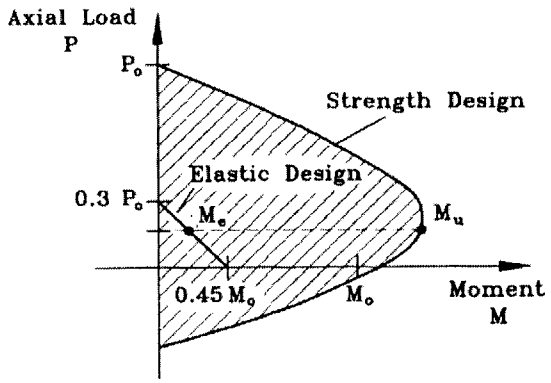

Figure 2-4: Typical column interaction diagram.

Elastic design was initially based on a linear relationship between axial load and moment, where a seemingly conservative value of 45% of the ultimate moment and 30% of the axial load was used, as shown in Figure 2-4. Because highway bridge columns are typically subjected to relatively low axial loads, the required flexural strength derived from the elastic interaction curve tended to be insufficient for flexure developed during seismic loading. However, conservative safety factors employed in elastic design in addition to unexpected increased material strength, such as strain hardening in steel reinforcement, led to unanticipated column strength in elastic design. Thus, the actual discrepancy between points M_e and M_u in the figure is smaller than implied by the design interaction curve. While elastic design has resulted in unforeseen column flexural strength, inadequacies exist in the fact that the columns lack ductile detailing provisions required for the satisfactory dissipation of energy [1]. Furthermore, the strength resulting from elastic design has been unanticipated and thus inconsistent, evident in the failure of numerous bridge columns and piers during recent earthquakes. Increased elastic design strength also affects shear failure, which will be described in detail below.

2.3.1.2 Undependable Column Flexural Strength

Not only has the elastic design methodology produced columns that possess inadequate flexural strength, but column strength is also undependable, due primarily to the design of longitudinal reinforcement. Failures due to reinforcement inadequacy most often result from insufficient development length of longitudinal rebar that is lap-spliced

just above the column footing [1]. The potential for plastic hinge development at this location warrants an increase in flexural strength, and many existing column designs have specified lap-splice lengths that are too short. Because the lap-splice lengths have proven to be insufficient for the necessary ductility levels required for energy dissipation, the column is unable to develop its full flexural strength. Butt-welds have also resulted in similar column failure when the splice is located just above the footing where significant moments tend to develop during seismic events. Since the strength and ductility of welds are difficult to guarantee, concentric flexural reinforcement welded at the same critical location within a column is prone to seismic failure.

2.3.1.3 Inadequate Flexural Ductility

Ductility, a controlling parameter in seismic design, can be defined as the ability of a structural member to experience significant plastic deformations without failing after the elastic yield point has been exceeded. Ductility is clearly an important consideration in earthquake design, as either a steel or reinforced concrete member must experience cyclic deformation and still retain adequate flexural capacity to avoid total collapse [6]. Ductility, μ, is measured in terms of multiples of yield displacement, and can be defined as

$$\mu = \frac{\Delta_m}{\Delta_y}$$

where Δ_m is the maximum displacement of the structural member when subjected to external loading, and Δ_y is the yield displacement of the member.

Failures due to insufficient ductility tend to be sequential, and failure is generally instigated at ductility levels of between 2 and 3, when plastic hinges begin to develop [1]. Strains in this region exceed the unconfined compression strength of concrete, and spalling of the external concrete cover begins to occur. If the column lacks adequate confinement in the form of hoop or spiral reinforcement, then the concrete column core will begin to crush as strains exceed the confined strength of the column. Complete failure of the column and collapse of the bridge structure becomes imminent as the column can no longer support the axial load from the bridge superstructure.

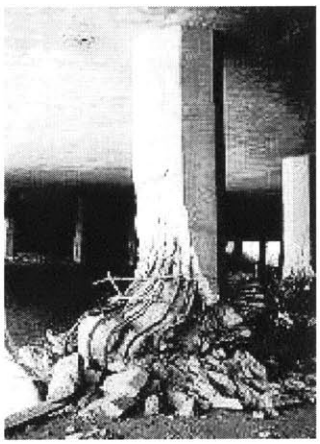

Figure 2-5: Flexural plastic hinge development.

Failure due to inadequate flexural ductility is shown above in Figure 2-5 [2]. This bridge column, subjected to the 1994 Northridge earthquake in California, exhibits flexural failure at the location of the plastic hinge development at the column base. The inadequate transverse reinforcement that decreased the confinement capacity and contributed to the column flexural failure can be noted in the figure.

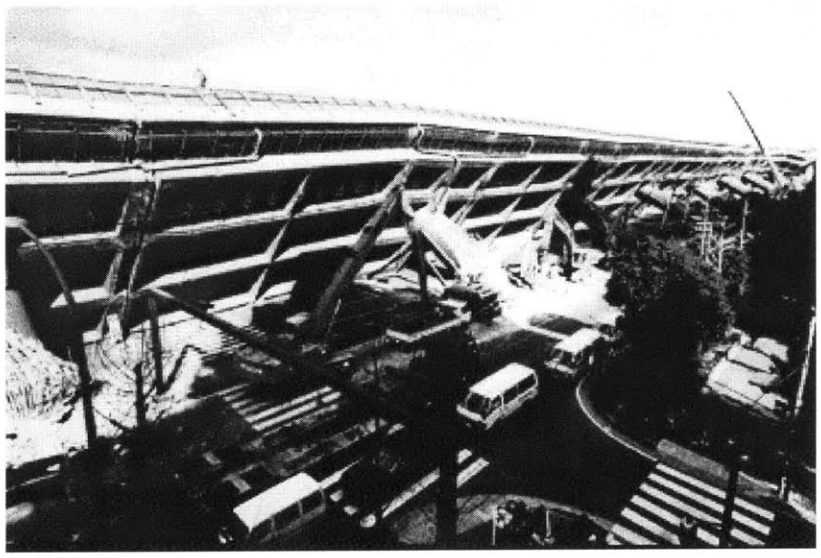

Figure 2-6: Collapsed Hanshin Expressway.

2.3.1.4 Premature Termination of Column Reinforcement

Premature termination of longitudinal column reinforcement creates a shear-flexure failure mechanism at mid-column height when the bridge structure is subjected to

seismic excitation. This failure mechanism can be quite devastating, as it is responsible for the infamous collapse of Japan's Hanshin Expressway during the 1995 Kobe earthquake. The collapsed expressway structure is shown above in Figure 2-6 [7]. In observed failures, flexural reinforcement termination within the column member was based on the expected location of maximum and minimum bending moments in the column. However, effects of tension shift due to diagonal cracking can result in a change of shape of the moment envelope, and maximum moments can then occur at the location of the terminated reinforcement, resulting in a combined flexural-shear column failure [1]. In addition, the location of termination of the reinforcement can shift the formation of the plastic hinge from the base toward the center of the column. Since the column base is more robustly confined than the column center, strains resulting from the formation of a plastic hinge at the column center exceed the confinement capacity of the concrete at this location, and failure ensues as described in the preceding section.

2.3.2 Column Shear Failure

Reinforced concrete columns resist shear through a variety of mechanisms, including direct cross-sectional effects, aggregate interlock in the cracked section, dowel action of the flexural reinforcement, and global transfer mechanisms such as the thrust, or arch mechanism [8]. The various shear mechanisms share a complex relationship, and as a result, shear failure cannot be controlled in the same manner as flexural failure. Ductility is utilized to control the flexural failure mechanisms of columns, but shear failure tends to be brittle and thus shear failure mechanisms are consequently immediate and explosive.

The simplest and most common shear failure mechanism in columns is characterized by the failure of transverse shear reinforcement. The failure of the reinforcement leads to subsequent decreased concrete confinement strength and ensuing failure under axial loads [1]. Shear failure tends to be most problematic in short columns since shear values are often greater than moment values in shorter members. Historically, shear failure resulting from seismic excitation is more prominent in bridges designed using an elastic philosophy for various reasons. First, shear failure mechanisms tended to be disregarded in elastic design, as many bridges, particularly in California,

were designed with the same shear reinforcement scheme, regardless of column geometry or anticipated seismic shear force. Second, conservatism in elastic design for flexural strength, discussed above, resulted in greater than expected elastic yield strengths, and columns consequently failed in shear as opposed to bending.

Observations following failures during earthquakes based on failure characteristics and the geometry of columns have resulted in the significant conclusion that the shear capacity of plastic hinge regions is smaller than that of non-plastic hinge regions. Flexural ductility causes an increase in the width of flexure-shear cracks, which in turn decreases the effectiveness of the aggregate interlock shear transfer mechanism [1]. Thus, it is important for designers to recognize the negative effects of increased ductility and flexural capacity on the column shear strength.

The typical shear failure mechanism is shown below in Figure 2-7 [9]. The column in the figure represents another failed bridge column in the 1994 Northridge earthquake in California. The column design includes a tapered cross-section at the top to presumably increase shear capacity at the column-superstructure interface. The stiffer top, however, forced shear failure to occur at the base of the taper where both a discontinuity in column stiffness and weaker confinement reinforcement exist.

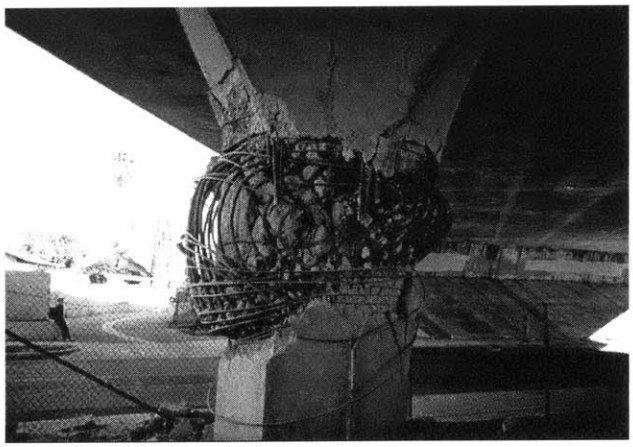

Figure 2-7: Shear failure mechanism.

2.4 The Seismic Isolation Remedy

It is evident from the above discussion that seismic forces cause extensive damage to simple span bridge structures. Damages from column failures and displacements are

severe, often resulting in the complete destruction of the structure. While the elastic design methodology has resulted in the seismic destruction of numerous bridges, inelastic design still proves to be inadequate, as unexpected failures have occurred during seismic events within the past decade to bridges specifically designed to resist powerful earthquakes. Additionally, inelastic design relies on local damage for energy dissipation to maintain structural integrity and to prevent collapse.

The implementation of seismic isolation systems in bridges can prevent the extensive damage described above. The decoupling of the deck superstructure from the supporting column substructure reduces absolute acceleration induced by the seismic excitation, and column damage is avoided. Relative displacements at the isolated superstructure level increase, but the elastic properties of the isolation bearings allow for significant displacements, and the displacement failures described above are avoided. A detailed description of the bearing mechanics and behavior of the isolated structure is found in the following chapters.

CHAPTER 3: STRUCTURAL BEHAVIOR

3.1 Introduction

This chapter examines the general structural behavior of base isolated structures. First, earthquake response spectra and their relationship to seismic isolation systems are analyzed. Next, the effects of structural stiffness on acceleration and relative displacement in response to lateral ground excitation are discussed. This discussion is then applied to the period shift of isolated structures, and corresponding advantages and disadvantages of the period shift are examined. Finally, the effectiveness of seismic isolation is emphasized through an investigation of ductility demand in earthquake resistant design.

3.2 Response Spectra Analysis

In order to gain an appreciable understanding of the beneficial effects of seismic isolation, traditional earthquake response spectra will be examined in detail. Studying spectral displacement and spectral acceleration offers insight into the dominant excitation frequency of a particular seismic event and consequential relative structural displacements and absolute accelerations that induce detrimental shear forces within structural members.

Response spectra illustrate the maximum response of a single degree of freedom (SDOF) system to a particular earthquake excitation in terms of either the frequency or natural period of the structural system. Moreover, for a particular seismic excitation, the absolute acceleration and relative displacements are proportional at any time, as the two response measures share identical time histories [10]. Response spectra are limited in that they depict SDOF systems, but bridge piers can be approximated as SDOF systems with the mass of the superstructure dead load lumped at the top of the supporting pier. The spectra can be used for approximate structural design, but will be used in this discussion for conceptual illustration purposes and will also be used in the Chapter 7 analysis of the structural behavior of an isolated structure.

Shown below in Figure 3-2 and Figure 3-3 are the spectral displacement and spectral acceleration response spectra for the 1994 Northridge, California earthquake

[11]. The response spectra include damping values of 0%, 2%, and 5% of critical damping. The earthquake ground acceleration time history, depicted in Figure 3-1, was obtained from Sylmar County Hospital at an orientation of 90 degrees. For spectral displacement, it is evident that dominant excitation periods occur at just under 1 s and again at approximately 2.5 s, while for absolute acceleration, the dominant excitation period occurs over a one-half second range centered at approximately 0.5 s. Thus, structures with natural periods below 2.5 s were most likely subjected to extreme acceleration and relative displacement during this seismic event.

While each earthquake is unique, the data from the Northridge earthquake shown below represents the general expected structural response to earthquakes in addition to the typical fundamental periods at which peak relative displacement and acceleration occur. This excitation period can prove troublesome for simple span bridges, and the applicability of these figures to the mechanics of seismic isolation will be discussed in detail below.

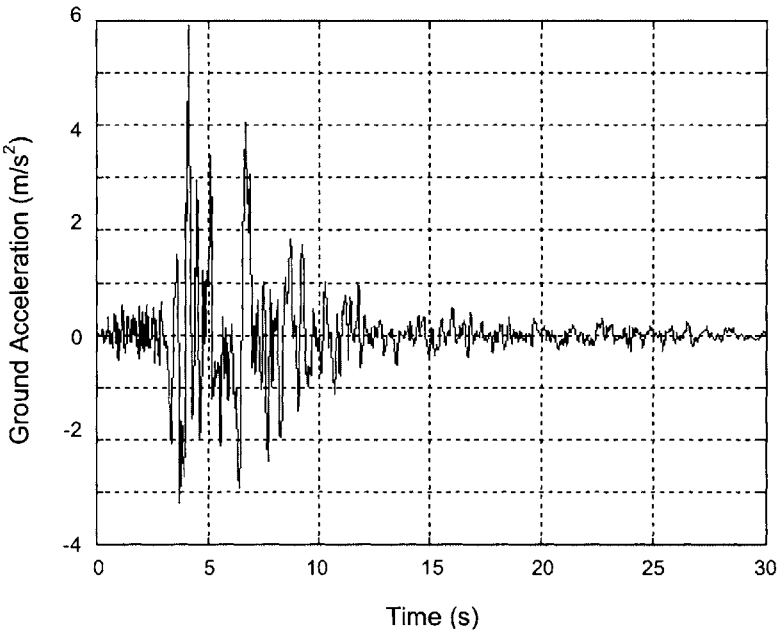

Figure 3-1: Ground acceleration time history – 1994 Northridge earthquake.

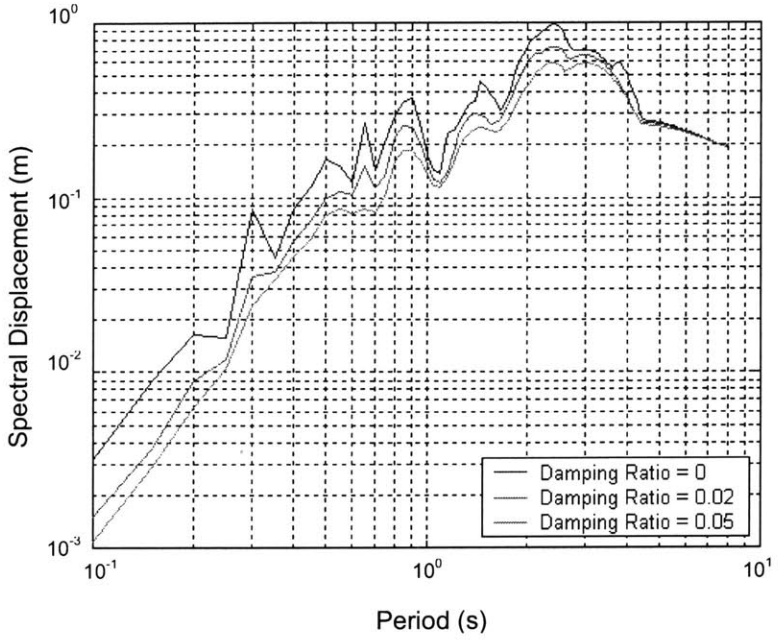

Figure 3-2: Spectral displacement – 1994 Northridge earthquake.

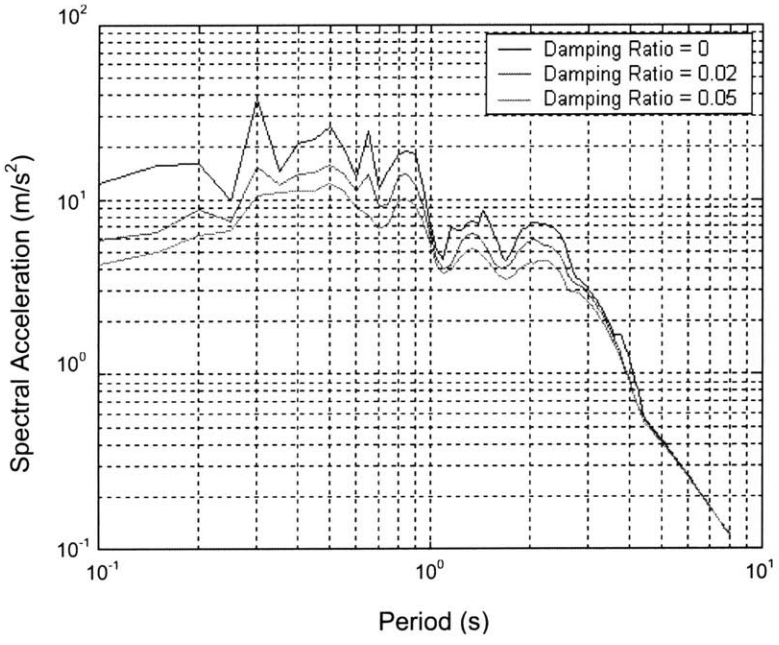

Figure 3-3: Spectral acceleration – 1994 Northridge earthquake.

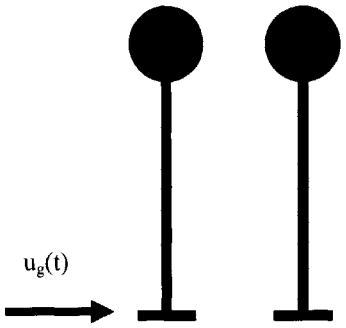

Figure 3-4: Infinitely rigid structure subjected to ground motion.

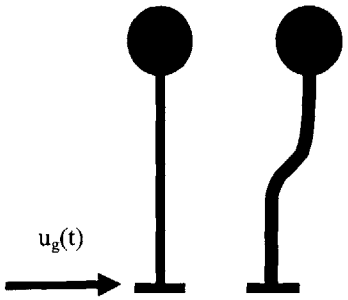

Figure 3-5: Negligibly rigid structure subjected to ground motion.

3.3 Effects of Stiffness on Fundamental Frequency

It was established in the previous section that structures possessing relatively low natural periods, such as simple span bridge structures, are in the dominant range of the earthquake excitation frequency. The behavior of the structure in response to seismic loads is a direct function of the fundamental frequency, which is in turn dependent upon the stiffness of the structure. The effect of structural stiffness on the fundamental frequency of the structure and corresponding response to lateral ground excitation are discussed in this section.

The effect of ground excitation upon structural behavior is illustrated above in Figure 3-4 and Figure 3-5. In Figure 3-4, an infinitely rigid structure is subjected to lateral ground excitation. Because of the infinite stiffness of the structure, the absolute acceleration of the mass at the top of the structure is equal to the acceleration of the ground. While no relative displacement occurs, the acceleration in the structure and the corresponding shear force in the column may exceed design limitations. Conversely, a

structure with negligible lateral stiffness subjected to horizontal support excitation is illustrated in Figure 3-5. In this scenario, the displacement of the mass relative to the ground is equal to the maximum ground displacement. Because the mass remains stationary relative to the ground, no acceleration in the mass is induced, and the absolute acceleration is zero. Thus, no shear force is developed in the column. The relative displacement of the mass, however, may exceed design limitations.

It is evident that for a conventionally designed structure, either large relative displacements, in the case of extremely low lateral stiffness, or large absolute accelerations, in the case extremely high lateral stiffness, will result from horizontal support excitation. The consequences of design stiffness and corresponding natural period have been explored above in the examination of the displacement and acceleration response spectra, where the fundamental frequency of the structure can potentially be in the range of the seismic excitation, amplifying either absolute acceleration or relative displacement.

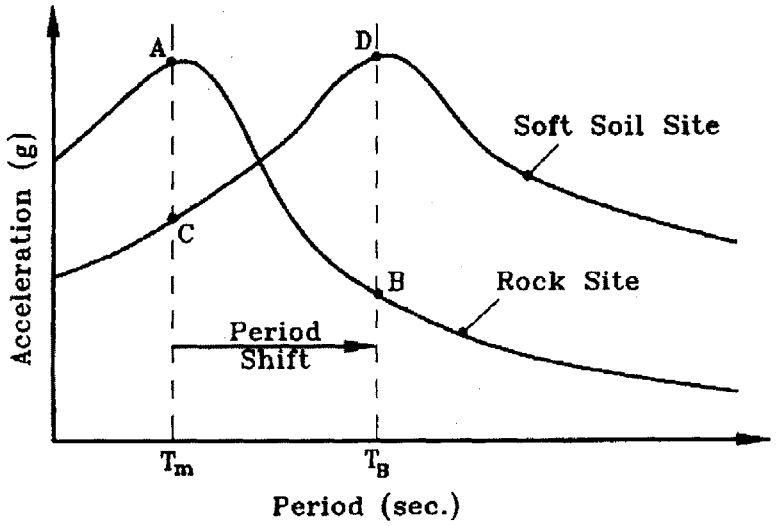

Figure 3-6: Illustration of the effect of natural period shift of isolated structures.

3.4 Period Shift

Clearly, it is most advantageous to limit absolute accelerations while reducing undesirable relative displacement. Both goals cannot be accomplished through

conventional structural design or through traditional construction materials, but the use of seismic isolation can greatly reduce absolute acceleration while limiting relative displacement to the isolated level. The reduction in absolute acceleration for a seismic isolated structure is effectively accomplished through a shift in the fundamental period of the structure. While this period shift is largely advantageous, several disadvantages are also inherent in the application of the shift in period. Specific advantages and disadvantages are discussed below.

3.4.1 Advantages

The effect of the shift of fundamental period of an isolated structure with respect to the acceleration response spectrum is shown above in Figure 3-6 [1]. The inclusion of a base isolation system in a structure decreases the effective stiffness of the structure and lengthens the corresponding natural period. The greatest advantage of the increase in period from T_m to T_B is a reduction in the absolute acceleration of the system, assuming the structure is founded on hard soil or rock and that there is no effect of soil conditions on seismic wave propagation. It is clear from the figure that the structural period is shifted away from the resonant acceleration location at point A to a location of lower acceleration at point B. This reduction in acceleration is particularly advantageous for bridge structures, where the majority of the mass is located at the superstructure level. If the superstructure is isolated, then the mass is no longer subjected to high levels of acceleration and subsequent shear forces in supporting columns and abutments are not developed.

3.4.2 Disadvantages

Several disadvantages also exist as a result of the shift in natural period of the structure that must be considered by the engineer in the implementation of seismic isolation. The first, most inconsequential disadvantage involves the actual necessity of seismic isolation in bridge structures. Most simple span highway bridges have natural frequencies in the range of seismic excitation, but bridge structures with long spans or with tall supporting piers may possess inherently long fundamental periods that are out of the range of earthquake excitation. In this case, seismic isolation is inapplicable, and the

only major consequence is a structure that could have been designed more efficiently and economically.

A second disadvantage of the period shift is the potential to increase absolute acceleration in the structure given the soil conditions at the site. The advantageous period shift discussed above assumes ground excitations that were not amplified by soil conditions at the site of the structure. It was assumed that the structure was founded on either rock or firm soil and that the acceleration response spectrum was unmodified from the initial earthquake excitation. If soft soil conditions exist at a particular site, earthquake waves are lengthened, and the peak period at which the maximum acceleration response is expected to occur increases. This is evident in Figure 3-6, where the peak response acceleration increases from point A to point D. If the period at which peak acceleration occurs for a given earthquake increases due to soil conditions, then it is clearly disadvantageous to increase the fundamental period of a structure that is already outside of the range of dominant seismic excitation, as absolute acceleration of the structure will increase. Thus, in the consideration of isolation systems for bridge structures, soil conditions and seismic excitation data at the bridge site must be carefully investigated, although bridges are usually not founded on soft soil.

A third disadvantage of the period shift is related to the relationship between increased relative displacements and the modified dynamic shape of the first mode. As illustrated above in the simplified stick model of Figure 3-5, a decrease in absolute acceleration, which occurs when the natural period of the structure increases, is accompanied by an increase in relative displacement. While this displacement is confined to the isolated level of the structure, it can be disadvantageous if supporting bridge columns or the column-bearing-superstructure interface are improperly designed. Only the first mode of vibration of the structure contributes to the overall behavior of the isolated structure, and the first mode is characterized by the deflection of only the isolated portion of the structure. Excessive deflections of the superstructure during seismic response shift the center of mass of the superstructure away from the center of the pier, resulting in an eccentric axial load. This eccentric load induces bending moments in the columns that can cause significant damage to members incapable of resisting flexural stress, leading to the possible collapse of the structure.

3.5 Ductility Demand and Seismic Isolation

The advantages of period shift discussed above are made even clearer when applied to a design spectrum, shown below in Figure 3-7 [12]. While acceleration response spectra show peak pseudo-accelerations for a given structural period, design spectra account for uncertainties associated with the estimation of fundamental structural period and the characteristics of earthquake excitation. These uncertainties are addressed by adding the standard deviation of multiple response spectra accelerations to the mean acceleration to produce a strength demand curve [13].

The design spectrum of Figure 3-7 illustrates the strength demand curve for a non-isolated bridge structure, the probable design strength of the non-isolated structure, and the ductility demand for the structure. Additionally, the reduced lateral force on an isolated bridge structure and corresponding fundamental period are depicted in the plot. In this figure, equivalent lateral force, rather than response acceleration, is plotted against structural period, essentially creating the same envelope as an acceleration response spectrum.

Curve 1 represents the elastic demand of the non-isolated structure, or the recommended elastic design force for the worst probable earthquake. Curve 4 represents the recommended maximum elastic design force, which allows for a statistically determined amount of inelastic deformation. Curve 3 represents the probable structural strength under the assumption that the structure has been conservatively designed to a certain extent. The difference between curve 1 and curve 3 represents the amount of force that causes inelastic deformation and that must be absorbed by the ductility of the structure. As discussed in Chapter 1, elastic bridge design results in severe damage due to increased structural stiffness and mass that increases lateral seismic forces and column shear. Thus, the strength design curve is located well below the capacity curve. After the strength capacity of the structure has been exhausted, earthquake energy must be dissipated through the ductility of the structure. This energy dissipation occurs through inelastic structural deformation and yielding of structural members, causing plastic deformation and permanent damage. While complete collapse of the bridge structure can be avoided, the structure must be taken out of service for costly repair.

The beneficial effects of seismic isolation and the increase in fundamental structural period are evident in the figure. Curve 2 represents the force on the isolated bridge structure, namely shear forces developed in the columns and abutments. This curve was developed assuming a significant amount of damping from the isolation system to facilitate the dissipation of energy. It is apparent in the figure that the isolated structure theoretically experiences no inelastic deformation since the force imposed on the isolated structure, represented by curve 2, is located below the probable strength curve, represented by curve 3. Thus, properly designed seismic isolation systems either significantly reduce or altogether eliminate the ductility demand of the structure. This situation is valid only for structures with an increased natural period that is out of the range of maximum ground acceleration.

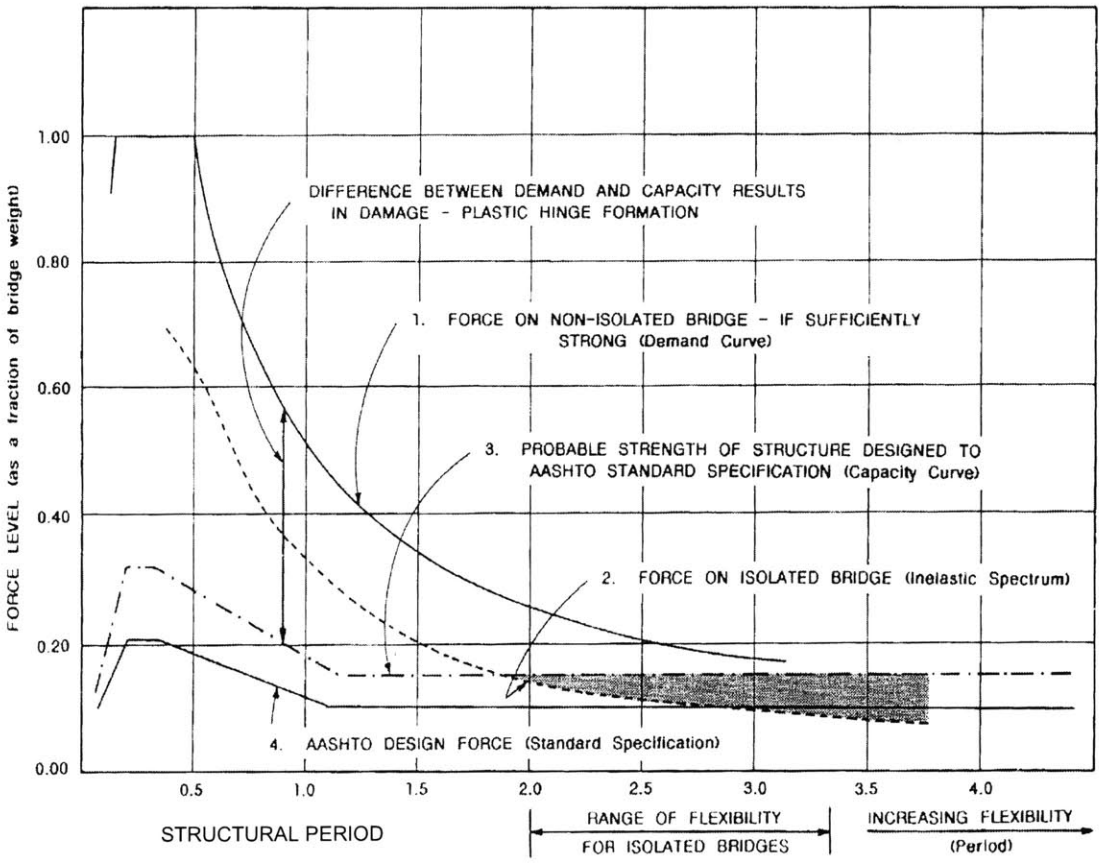

Figure 3-7: Effect of period shift with respect to conventional design spectrum.

CHAPTER 4: COMPONENTS OF ISOLATION SYSTEMS

4.1 Introduction

Because the concept of seismic isolation has been in practical use and development for the last three decades, the technology is mature and numerous isolation schemes exist. The most common isolation schemes used in bridge structures are elastometric systems and sliding systems. Both systems are essentially comprised of isolator bearings used in combination with initiating and limiting devices, if required. Both isolation systems also have inherent damping properties and are employed to shift the fundamental frequency of the structure out of the range of harmful seismic excitation, thus reducing acceleration and corresponding column shear. Unique characteristics are exhibited by the different isolation schemes within the two respective categories. Such defining characteristics include initial stiffness and subsequent deformation under service loads, yield force and total displacement under extreme earthquake loads, the re-centering ability of the system, and vertical stiffness [14]. The most prevalent features of each isolation system will be addressed in this section.

4.2 Elastometric Systems

Elastometric systems are characterized by their name, as their effectiveness is derived from their composition of elastometric material. Commonly employed elastometric systems include natural rubber bearings, lead-rubber bearings, and high-damping natural rubber bearings. The specifics of these systems are discussed in detail below.

4.2.1 Natural Rubber Bearings

Natural rubber bearings, also known as laminated rubber bearings, can be manufactured using either natural rubber or neoprene, a synthetic rubber material utilized for its toughness and durability that behaves in a similar manner to natural rubber [15]. As shown below in Figure 4-1 [14], the bearings are manufactured in alternating layers of rubber and thin steel shims. The shim and rubber layers are vulcanized in a mold under heat and pressure in a single process to produce the composite bearing. The shims

provide stiffness in the vertical direction and prevent the bulging of the elastometric material when significant axial loads are applied to the bearings. This vertical stiffness is also required to prevent a rocking response when the structure is subjected to seismic excitation. The steel shims have no effect upon lateral stiffness, which is controlled by the shear modulus of the elastometric material and the allowable shear deformation of the structure. The entire system is mounted between thick steel endplates to facilitate the connection between the isolated and non-isolated portion of the structure.

The primary disadvantage of natural rubber bearings is the necessity for auxiliary damping devices. Natural rubber bearings are considered low-damping devices because they exhibit relatively small damping values of approximately 2-3% of critical damping. Damping can be controlled to a limited extent by enhancing the material properties of the elastomer, but usually supplementary external damping devices, such as viscous dampers and hysteretic dampers, must be used in parallel with the bearings to aid in the control of motion under both low level service loads and extreme seismic loads.

There are, however, numerous advantages of natural rubber bearings. First, the bearings are easily manufactured and installed, especially in the seismic rehabilitation of bridge structures. Second, the bearings can be easily modeled and analyzed, and consequently easily designed. Finally, the effects of temperature, aging, loading rate, and creep upon the elastometric material are negligible, resulting in long term stability of the shear modulus and subsequent predictable behavior over time [3].

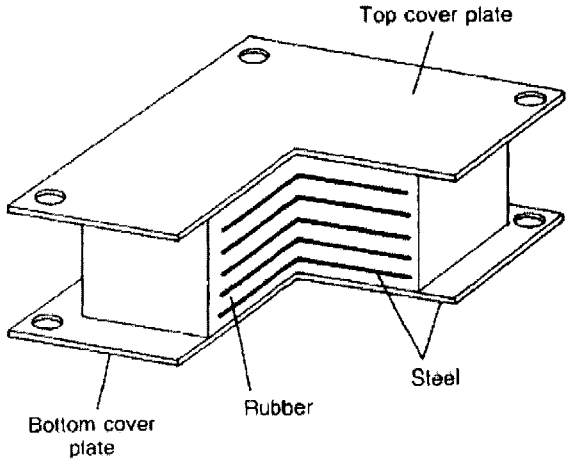

Figure 4-1: Natural rubber bearing schematic.

4.2.2 Lead-Rubber Bearings

The lead-rubber bearing, shown below in Figure 4-2 [14], was developed in response to the inadequate damping characteristics of the natural rubber bearing. The bearing is essentially identical to the natural rubber bearing except for the addition of a cylindrical lead "plug" located at the center of the bearing. The lead plug induces a bilinear response to high levels of lateral excitation, where the stiffness of the system decreases after the plug deforms inelastically in shear. Under service loads, the system gains its rigidity from the stiffness of the plug, and after the lead yields under seismic loads, the stiffness of the system is considerably reduced. The deformation of the plug after yielding results in the hysteretic dissipation of energy, and the amount of dissipated energy is a function of the allowable displacement of the bearing [3]. Lead rubber bearings share the same advantages of natural rubber bearings in terms of manufacturing, modeling and analysis, and implementation.

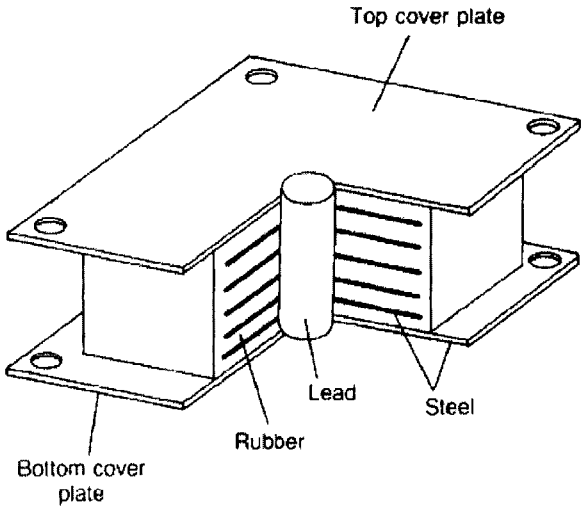

Figure 4-2: Lead-rubber bearing schematic.

4.2.3 High Damping Natural Rubber Bearings

High damping natural rubber bearing isolation systems were developed to eliminate the need for the extraneous supplementary damping devices required for natural rubber bearings while avoiding the discontinuous bilinear behavior of lead-rubber bearings. The bearings are similar in geometry to natural rubber bearings, and the only major difference between the two bearing types lies within the characteristics of the

natural rubber elastomer. Damping in the natural rubber is augmented through the addition of fillers such as carbon, oils, or resins. The addition of these fillers increases the isolator damping from 2-3% of critical damping to the range of 10-20% of critical damping.

At low shear strains of less than 20%, the high damping natural rubber bearing exhibits nonlinear behavior and is characterized by high stiffness and high damping, which limit deflections when the structure is subjected to service loads. As shear strains increase from 20% to 120%, the damping characteristics of the elastomer decrease, but the shear modulus remains constant. At strains greater than 120%, the shear modulus increases and is accompanied by an increase in damping. This behavior results in an advantageous system that exhibits adequate stiffness under service loads and that also limits displacements while dissipating energy under extreme earthquake loads.

In addition to ideal behavior under both lateral service loads and extreme loads, high damping natural rubber bearings also exhibit advantages related to implementation and vibration absorption. First, high damping natural rubber bearings can be manufactured using the same vulcanization process as natural rubber bearings and lead-rubber bearings, and can also be installed in the same manner as the aforementioned bearings. Second, the high damping natural rubber systems filter ambient vibrations from superstructure traffic or from adjacent spans, thus limiting vertical vibrations in the bridge deck [3].

4.3 Sliding Systems

Sliding isolation systems, like elastometric systems, effectively remove the structure from the dominant excitation period of the earthquake and possess several advantages over elastometric systems. First, sliding systems are less sensitive to the dominant excitation period of the earthquake, and energy is effectively dissipated over a range of earthquake excitations. Second, because the frictional force mobilized in sliding systems is both proportional to the mass of the structure and is developed beneath the isolated portion of the structure, the center of mass of the structure coincides with the center of resistance of the sliding system. Thus, torsional effects in structures that are asymmetric in either geometry or stiffness are avoided [14]. Commonly employed

sliding systems include pure friction systems, resilient-friction base isolation systems, and friction pendulum systems. The specifics of each isolator scheme are examined in detail below.

4.3.1 Pure Friction Systems

The pure friction system is the earliest and simplest sliding isolation scheme and best represents the principles of sliding isolation systems. The system utilizes a sliding joint to decouple the superstructure from the substructure and operates under the principle of sliding friction [14]. At low lateral service loads, the entire structure acts as a fixed-base system since lateral forces are too insignificant to overcome the static frictional force and induce horizontal displacement. When the system is subjected to significant lateral seismic forces, the frictional force is overwhelmed and sliding is mobilized. Accelerations in the structure are reduced through the dissipation of energy through friction in the form of Coulomb damping. The lateral force required to overcome the static frictional force is a function of the coefficient of static friction and can be controlled through the selection of material to be employed at the bearing surface. Clear disadvantages of the system include continuous maintenance of the bearings to ensure a constant coefficient of friction and the inability of the system to re-center after an extreme event.

4.3.2 Resilient-Friction Base Isolation Systems

The resilient-friction base isolation system is depicted below in Figure 4-3 [14]. The behavior of the system is largely frictional in nature, but the bearings make partial use of the properties of elastometric bearings. Resilient friction base isolation bearings are comprised of thin sliding plates surrounding an elastometric core and mounted between two end plates. The multiple sliding plates, coated in Teflon or stainless steel, help to ensure a relatively low frictional coefficient and the avoidance of large accelerations under relatively significant lateral forces. The frictional force that develops between plates is large enough so that motion is not induced under the application of lateral service loads. The concentric layers of plates surround a central rubber core, and often times smaller peripheral rubber cores are also inserted in the isolation bearing.

These elastometric plugs store strain energy during seismic excitation and provide an elastic restoring force to re-center the bearings when the lateral seismic forces have subsided. As in the case of the pure friction system, energy is consistently dissipated through Coulomb damping [3].

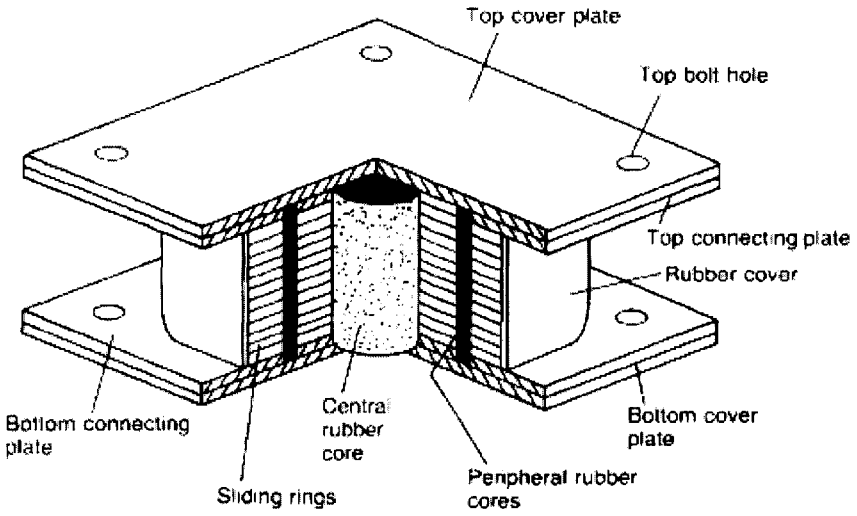

Figure 4-3: Resilient-friction base isolation system bearing schematic.

4.3.3 Friction Pendulum Systems

The friction pendulum system, illustrated below in Figure 4-4 [14], combines the concept of sliding isolation systems with the action of a pendulum. The superstructure is isolated form the substructure via a bearing that is comprised of an articulated slider resting on top of a convex bearing surface with a low coefficient of friction, usually made of chrome [14] or stainless steel [3]. When lateral seismic forces overcome static friction, the articulated slider is displaced along the convex spherical bearing surface. If friction between the articulator and the bearing surface is neglected, then the system behaves as a simple pendulum. The restoring force that re-centers the friction pendulum system is provided by the change in direction of the frictional and normal forces as the articulator slides up the wall of the curved bearing surface. Coulomb damping generated through sliding friction provides constant energy dissipation in the bearing. The effective stiffness and subsequent shifted period of the isolated system, based on the dynamics of a pendulum, is dependent upon the radius of curvature of the convex bearing surface [14].

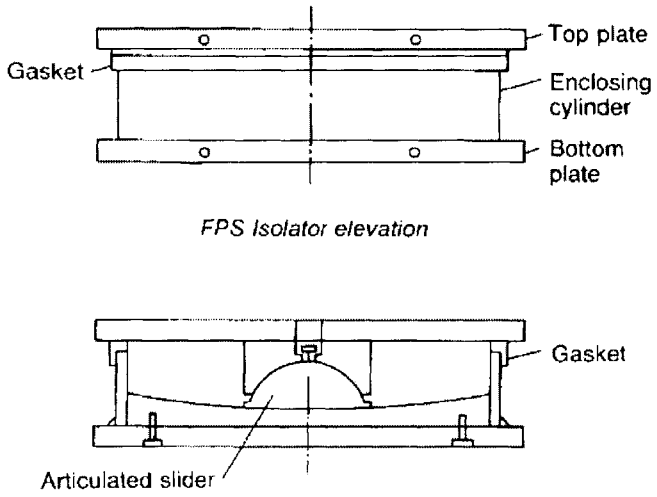

Figure 4-4: Friction pendulum system isolator bearing schematic.

4.4 Initiating and Limiting Devices

Induced deformations in the isolation devices described above are initiated by significant seismic forces, and maximum relative displacements are controlled to an extent through the design and inherent material characteristics of the bearings. However, supplementary initiation and limiting devices are sometimes required to further control the relative displacements of the isolated structure [14].

Systems that are too flexible under lateral service loads often require an initiating device, such as a shear key, to provide increased stiffness and to also act as a fuse when the structure is subjected to considerable seismic excitation. Major problems that exist with initiating devices include local damage and the creation of a significant stiffness discontinuity in the isolation system. Localized damage must be addressed through inspection and repair after a seismic event and could eventually offset the cost effectiveness of the isolation system. The creation of a major discontinuity in the stiffness of the structure can lead to the excitation of higher modes during an earthquake, resulting in increased relative displacements and accelerations.

During improbable extreme seismic events, limiting devices may be required to control the deflection of the isolated superstructure. Elastometric bearings are

particularly prone to problems with excessive deformation, as they may become unstable under significant strains. Additionally, pounding against adjacent structures could occur with excessive displacements, resulting in increased column shear forces and the potential for localized damage, especially in the case of reinforced concrete structures. Either rigid or deformable devices can be used to limit deflection, but once deflection is constrained, accelerations in the structure may increase, or local damage to the limiting device may occur. The implementation of a system that optimally reduces acceleration, relative displacement, and local damage is ultimately in the hands of the designer.

CHAPTER 5: MECHANICS OF ELASTOMETRIC BEARINGS

5.1 Introduction

The concept of seismic isolation is relatively straightforward, but the realization of isolation lies within the sophisticated mechanics of the isolation devices. The systems must possess both vertical and lateral stiffness tailored to the applied loads and geometry of the structure, where the isolators are sufficiently stiff to resist service loads but flexible enough to significantly deform under seismic excitation. Isolators must also have sufficient energy dissipation mechanisms.

Isolation bearings must be significantly stiff in the vertical direction in order to reduce the potential for structural rocking under eccentric vertical loads. In simply supported bridge structures, eccentric traffic loads can induce oscillations about the longitudinal axis of the bridge if isolators do not possess sufficient vertical stiffness. Isolators must also be sufficiently rigid when subjected to lateral service loads. Such loads include horizontal wind forces that can induce cyclic vibration if vortex shedding about the superstructure occurs and longitudinal forces from vehicle braking and acceleration. The isolators, of course, must also possess adequate flexibility in the lateral direction in order to allow for significant relative displacement when subjected to seismic excitation. This relative displacement permits the shift in fundamental frequency that effectively removes the structure from the range of the dominant earthquake excitation frequency.

Efficient isolation systems must dissipate energy as well as possess sufficient stiffness. The ideal isolation system can continuously dissipate energy under both service loads and intense seismic loads, and this energy is arguably most efficiently dissipated through viscous and hysteretic damping mechanisms. Viscous damping allows for continuous energy dissipation under lateral service loads and both minor and severe seismic excitations. Viscous damping alone cannot provide sufficient energy dissipation for severe impulsive excitations, and additional dissipation is required, ideally in the form of hysteretic damping. Hysteretic damping, provided through the inelastic deformation of a low-yielding metal, provides high stiffness under service loads and high damping under severe excitation. While the damping mechanism provided by hysteretic dampers

is beneficial under extreme lateral loads, it creates a discontinuity in the stiffness of the isolation system. This sudden change in stiffness has the potential to increase the absolute acceleration of the isolated structure in the transition from minor to severe lateral excitation.

5.2 Modeling of Bearings

Since elastometric bearings are most commonly implemented in the seismic isolation of bridge structures, they will be discussed in detail in this section. The most common types of bearings used are natural rubber bearings and lead-rubber bearings, both of which were discussed in the previous chapter. Lead-rubber bearings are more commonly used than natural rubber bearings, but an overview of the modeling of natural rubber bearings will first be presented to illustrate both the advantageous properties of rubber and the necessity for the inclusion of the hysteretic lead element. The more common lead-rubber bearing will then be presented to illustrate the effectiveness of the bilinear system that incorporates hysteretic energy dissipation.

5.2.1 Natural Rubber Bearings

Rubber is a viscoelastic material and is capable of dissipating moderate amounts of energy without the inclusion of additional damping devices. Thus, the natural rubber bearing can perform satisfactorily as an isolation device. A detailed geometry and configuration of the natural rubber bearing has been described in the previous chapter. The following discussion highlights the mechanical behavior of the natural rubber bearing and relies upon that developed by Jerome Connor [16].

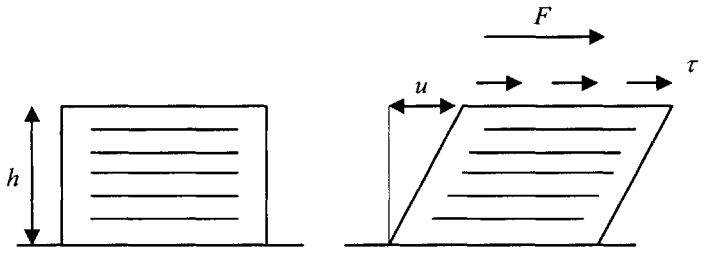

Figure 5-1: Natural rubber bearing in initial condition and deformed condition.

Given the aforementioned geometry, the natural rubber bearing can be rudimentarily modeled as a simple shear element, although nonlinearities exist in the system. The initial configuration and deformed configuration of the element is illustrated above in Figure 5-1 [16].

The shear strain, γ, of the bearing is defined as

$$\gamma = \frac{u}{h} \tag{5-1}$$

and the applied shear force, F, is defined as

$$F = \tau A \tag{5-2}$$

where τ is the shear stress and A is the cross-sectional area of the bearing. Assuming harmonic shear strain, the viscoelastic constitutive equations are

$$\gamma = \hat{\gamma} \sin \Omega t \tag{5-3}$$

and

$$\tau = G_s \hat{\gamma} \sin \Omega t + \eta G_s \hat{\gamma} \cos \Omega t \tag{5-4}$$

where G_s is the storage modulus of the rubber material, η is the loss factor of the rubber, and Ω is the forcing frequency. The storage modulus and loss factor are a function of the forcing frequency and temperature and can be determined from empirical material properties. For rubber material exhibiting high damping characteristics and subsequent nonlinear viscoelastic behavior, the storage modulus and loss factor are also dependent upon strain amplitude.

The stiffness and damping characteristics of the bearing can be derived from the linearized force-displacement relationship, defined by

$$F = k_{eq} u + c_{eq} \dot{u} \tag{5-5}$$

where k_{eq} and c_{eq} are the equivalent linear stiffness and viscous damping of the system. These two quantities can be obtained from the material properties of the elastomer by

using a least squares methodology [16]. The desired behavior of the isolation system can then be controlled through the geometric design of the isolation bearings.

5.2.2 Lead-Rubber Bearings

The necessity for additional energy dissipation in seismic isolation systems led to the development of the hysteretic damping mechanism in the lead-rubber bearing. The lead-rubber bearing provides all of the advantages of the natural rubber bearing, including vertical stiffness, horizontal flexibility to allow for the fundamental structural period shift, and inherent damping in the rubber. However, the addition of the lead plug provides additional initial stiffness under lateral service loads. More importantly, the lead plug provides hysteretic damping and subsequent energy dissipation under extreme seismic lateral loading, reducing both relative displacements and absolute acceleration in the isolated superstructure. Because of the added rigidity of the isolator, the rubber used in the lead-rubber bearing generally has both lower values of stiffness and inherent damping characteristics.

The physical properties of lead significantly affect the behavior of the isolation system and the subsequent overall behavior of the isolated structure. Because lead is a crystalline material, it changes structure temporarily when subjected to loads greater than its yield strength. Since the rubber that envelops the lead core remains elastic under significantly greater shear strains than lead, the original lead structural matrix is re-established once the applied lateral force is removed. The restoring force from the stored strain in the rubber re-centers the bearing into its initial equilibrium position [13].

Once the yield stress of the lead plug has been achieved, energy is dissipated hysteretically in the form of heat. The yield strength of lead in shear is approximately 10 MPa (1.5 ksi) [14], which is quite small in comparison to the yield strength in shear of structural steel, which is about 145 MPa (21 ksi). Thus, the isolators will deform inelastically and begin to dissipate energy long before structural members, such as supporting piers, begin to yield. The yield point of individual bearings and the lateral stiffness of the overall isolation system can be controlled through the dimensions of the lead plug. If the bridge is of irregular geometry, such that the torsional deformation mode is easily excited, then individual isolators within the system can be designed with

varying stiffness to ensure uniform displacement of the superstructure in either the longitudinal or transverse direction. The effects of torsional vibration will be explored further in the analysis in Chapter 7. Finally, lead generally resists fatigue, so extensive cyclic loading over the life of the bridge will not significantly reduce either the yield strength of the lead or its hysteretic dissipation properties.

The mechanical behavior of the lead-rubber bearing can be approximated with a bilinear stiffness model. The development of this bilinear model is illustrated below in Figure 5-2 [13]. In the figure, the simplified linearized force versus displacement relationship for each of the components of the lead-rubber bearing is plotted. The combined effective bilinear stiffness of the bearing system is also plotted. Figure 5-2 (a) represents the elastic stiffness of the rubber, assuming the applied force is below the yield point of rubber and that the rubber behaves linearly. The nonlinear nature of rubber was discussed above, but a linear approximation is qualified because the comparatively high stiffness of the lead plug controls the behavior of the bearing, with a stiffness nearly ten times that of rubber. The effective stiffness of the rubber can be approximated in the same manner as the natural rubber bearing, described in the previous section. The simplified elastic-plastic nature of the lead plug is shown in Figure 5-2 (b), where it is assumed that lead exhibits perfectly plastic behavior after the applied force has exceeded the yield strength of the lead plug. Finally, the combined stiffness of the lead plug and rubber bearing are shown in Figure 5-2 (c). It is evident that the elastic stiffness of the composite system is equal to the combined stiffness of the lead and rubber under low lateral loads, while the post-yield stiffness of the system is equal to only the stiffness of the rubber.

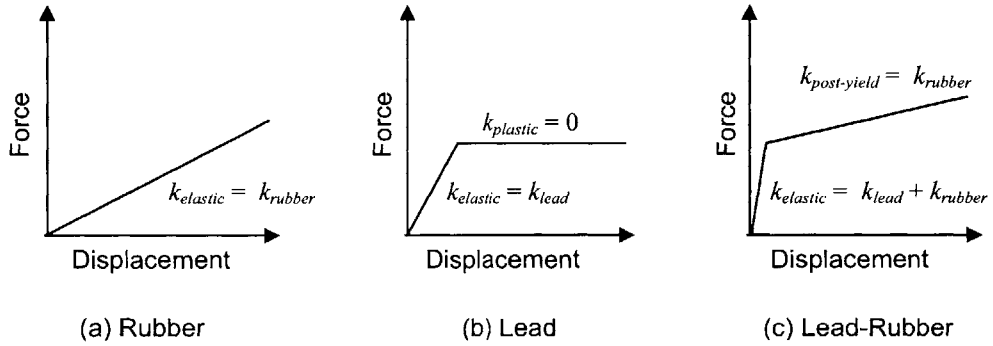

Figure 5-2: Bilinear stiffness development of the lead-rubber bearing model.

In Figure 5-3 [17], shown below, the effect of bilinear stiffness on the hysteretic characteristics of the isolator is illustrated. The solid lines signify the bilinear elastic and post-yield stiffness, described above, while the dashed parallelogram corresponds to the hysteresis loop. The area of the hysteresis loop represents the work done by the isolation device and is equivalent to the amount of energy dissipated. As explained above, the stiffness of the rubber material in the isolator is small in comparison to the stiffness of the lead plug. Thus, the dissipative properties of the isolator are primarily dictated by the characteristics of the lead plug, namely the yield force, F_y, and the corresponding yield displacement, u_y. Since the yield strength of lead is generally constant, the amount of energy dissipated and subsequent reductions in acceleration and relative displacement of the isolated structure depend upon the maximum allowable displacement of the isolation device, u_{max}. u_{max} is therefore an important design parameter and is a function of the permissible deflection of the isolated superstructure relative to adjacent fixed structures, such as bridge abutments and neighboring spans.

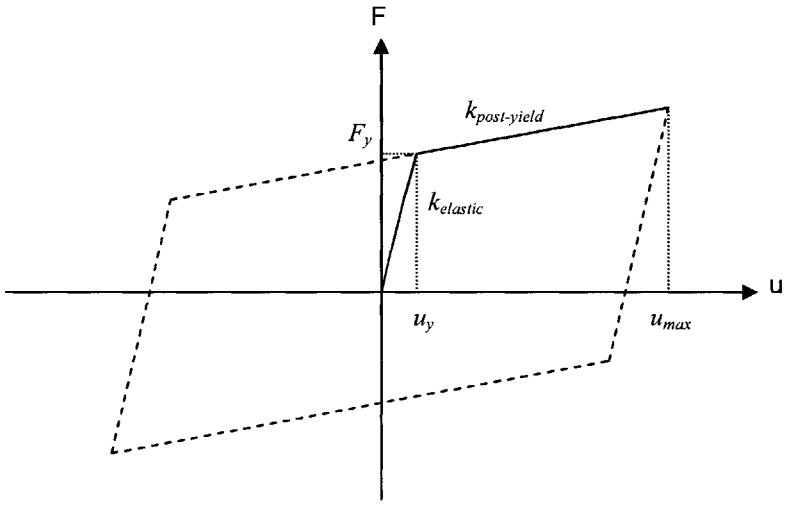

Figure 5-3: Force-displacement relationship and corresponding hysteresis loop for lead-rubber isolation bearings.

Fragiacomo et al., have studied the effect of the ratio of post-yield stiffness to elastic stiffness, defined as the bilinear stiffness ratio, upon structural behavior [17]. Their findings show that the optimal bilinear stiffness ratio is dependent upon both the characteristics of the earthquake excitation and the ratio of the isolated mass to the

structural mass. According to the study, for some earthquake excitations, isolation systems with comparatively low values of stiffness and high yield strength perform best, while for other excitations, systems exhibiting relatively high values of stiffness and low yield strength perform optimally. Because each earthquake excitation is unique, no trend can be developed. However, earthquakes occurring in a similar geographic region generally exhibit similar characteristics and comparable excitation frequencies. The study emphasizes the importance of consulting local data in the design of seismic isolation systems. Earthquake time-histories, in addition to the effects of soil conditions on seismic accelerations for the desired location of the seismic isolation system, must be utilized for effective base isolation system design.

CHAPTER 6: LINEAR THEORY

6.1 Introduction

It has been emphasized earlier that the predominant advantage of seismic isolation systems is a shift in the fundamental period of the structure away from the dominant period of earthquake excitation. Additionally, it has been previously discussed that the first dynamic mode of vibration of the structure consists of only the deformed shape of the isolated portion of the structure, and that only the first dynamic mode contributes to the development of internal structural forces. These considerations have been discussed in a qualitative sense, and the linear theory that describes the mathematic and physical behavior of seismic isolation systems will be examined in this section. The linear theory for the general case is outlined and is then simplified for the case of simple span bridges. The material presented in this chapter has been developed in detail by James Kelly [18].

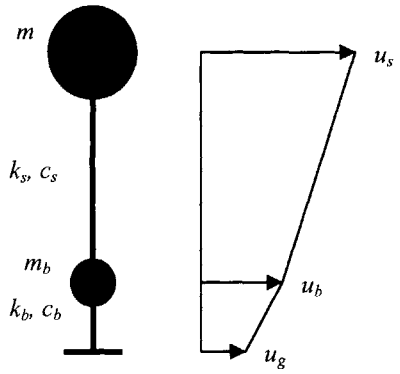

Figure 6-1: Parameters and assumed displacements of two DOF system.

6.2 General Case

The model presented above in Figure 6-1 [18] consists of a two degree of freedom (DOF) system with linear stiffness and linear viscous damping, and the ensuing discussion is developed based on this model. Although most isolation systems behave nonlinearly, the conclusions developed from the linear model in this discussion satisfactorily explain the general behavior of seismic isolation systems. In this model, the mass of the isolated portion of the structure is denoted by m and the mass at the level of the isolators is denoted by m_b. The stiffness and damping of the isolated structure are

denoted by k_s and c_s, respectively, while the stiffness and damping of the isolated level are denoted by k_b and c_b.

The absolute equations of motion derived from the above model are

$$m\ddot{u}_s = -c_s(\dot{u}_s - \dot{u}_b) - k_s(u_s - u_b) \tag{6-1}$$

and

$$m\ddot{u}_s + m_b\ddot{u}_b = -c_b(\dot{u}_b - \dot{u}_g) - k_b(u_b - u_g) \tag{6-2}$$

These equations can be expressed more conveniently in terms of absolute displacements, defined as

$$v_s = u_s - u_b \tag{6-3}$$

and

$$v_b = u_b - u_g \tag{6-4}$$

The equations of motion are rewritten as

$$m\ddot{v}_b + m\ddot{v}_s + c_s\dot{v}_s + k_s v_s = -m\ddot{u}_g \tag{6-5}$$

and

$$(m + m_b)\ddot{v}_b + m\ddot{v}_s + c_b\dot{v}_b + k_b v_b = -(m + m_b)\ddot{u}_g \tag{6-6}$$

These equations can be expressed in matrix form as

$$\mathbf{M}\ddot{\mathbf{v}} + \mathbf{C}\dot{\mathbf{v}} + \mathbf{K}\mathbf{v} = \mathbf{-M}\mathbf{r}\ddot{\mathbf{u}}_\mathbf{g} \tag{6-7}$$

where

$$M = m + m_b$$

$$\mathbf{M} = \begin{bmatrix} M & m \\ m & m \end{bmatrix} \qquad \mathbf{C} = \begin{bmatrix} c_b & 0 \\ 0 & c_s \end{bmatrix} \qquad \mathbf{K} = \begin{bmatrix} k_b & 0 \\ 0 & k_s \end{bmatrix}$$

$$\mathbf{v} = \begin{bmatrix} v_b \\ v_s \end{bmatrix} \qquad \mathbf{r} = \begin{bmatrix} 1 \\ 0 \end{bmatrix}$$

To simplify the analysis, several assumptions are applied. First, it is assumed that $m_b < m$, but the masses are of the same order of magnitude. Second, in terms of the frequencies of the two portions of the structure, it is assumed that $\omega_s >> \omega_b$, and $\varepsilon = (\omega_s/\omega_b)^2$ is of the order of magnitude of 10^{-2}. Finally, the system damping factors, ξ_s and ξ_b, are also of the order of magnitude of 10^{-2}.

The undamped natural modes of the system are denoted as

$$\boldsymbol{\varphi}^n = \begin{bmatrix} \phi_b^n & \phi_s^n \end{bmatrix}^T \qquad n = 1,2$$

These modes are implicitly defined as

$$\left(-\omega_n^2 + \omega_b^2\right)\phi_b^n + \left(-\gamma\omega_n^2\right)\phi_s^n = 0 \tag{6-8}$$

and

$$\left(-\omega_n^2\right)\phi_b^n + \left(-\omega_n^2 + \omega_s^2\right)\phi_s^n = 0 \tag{6-9}$$

where ω_n is the mode frequency and $\gamma = m/M$ is the mass ratio.

The characteristic equation for ω_n is defined as

$$(1-\gamma)\omega_n^4 - \left(\omega_b^2 + \omega_s^2\right)\omega_n^2 + \omega_b^2\omega_s^2 = 0 \tag{6-10}$$

Solving the characteristic equation while considering the fact that $\omega_s >> \omega_b$ and utilizing binomial series expansion to obtain a solution of the same order as ε results in the following solution for ω_1 and ω_2, the first two modal frequencies

$$\omega_1^2 = \omega_b^{*2} = \omega_b^2\left(1 - \gamma\frac{\omega_b^2}{\omega_s^2}\right) \tag{6-11}$$

and

$$\omega_2^2 = \omega_s^{*2} = \frac{\omega_s^2}{1-\gamma}\left(1+\gamma\frac{\omega_b^2}{\omega_s^2}\right) \tag{6-12}$$

It can be noted that ω^*_b is the lower of the two roots and represents the shifted isolation frequency while ω^*_s is the greater of the two roots and represents the modified frequency of the structure. Because the change in isolation frequency of the structure is of order ε and the frequency of the structure is considerably increased by the base mass, ω^*_b and ω^*_s can be approximated as

$$\omega_b^* = \omega_b \tag{6-13}$$

and

$$\omega_s^* = \frac{\omega_s}{\sqrt{1-\gamma}} \tag{6-14}$$

The two mode shapes, ϕ^1 and ϕ^2, can be obtained from equations 6-8 and 6-9 by retaining terms of order ε and by setting $\phi_b{}^1$ equal to 1.

$$\phi^1 = \begin{bmatrix} 1 \\ \varepsilon \end{bmatrix} \tag{6-15}$$

and

$$\phi^2 = \begin{bmatrix} 1 \\ \dfrac{[1-(1-\gamma)\varepsilon}{\gamma} \end{bmatrix} \tag{6-16}$$

These two mode shapes are plotted below in Figure 6-2 [18]. In the first mode shape, the isolated portion of the structure is nearly rigid, considering that ε is small compared to one and even smaller compared to the isolated structure height. In the second mode shape, it can be observed that the two masses, m_s and m_b, vibrate nearly

freely about the center of mass of the structural system. This vibration shape implies that negligible base shear is developed due to large accelerations in the second mode.

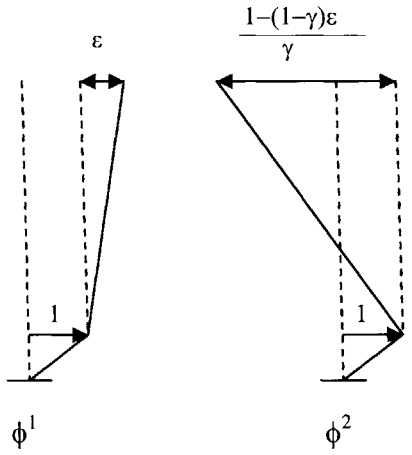

Figure 6-2: First and second mode shapes of the isolated system.

The relative displacements, v_b and v_s, defined by equations 6-3 and 6-4, can be written in terms of ϕ^1 and ϕ^2 as

$$v_b = q_1\phi_b^1 + q_2\phi_b^2 \tag{6-17}$$

and

$$v_s = q_1\phi_s^1 + q_2\phi_s^2 \tag{6-18}$$

The equation of motion, written above in matrix form in equation 6-7, becomes

$$\ddot{q}_1 + 2\omega_b^*\xi_b^*\dot{q}_1 + \omega_b^{*2}q_1 = -L_1\ddot{u}_g \tag{6-19}$$

and

$$\ddot{q}_2 + 2\omega_s^*\xi_s^*\dot{q}_2 + \omega_2^{*2}q_2 = -L_2\ddot{u}_g \tag{6-20}$$

In this formulation, the damping in the structural system is assumed to be small enough to retain orthogonality of the modes with respect to each other and the ground motion. L_1 and L_2, the participation factors, are defined as

$$L_n = \frac{\phi^{n^T}\mathbf{M}\mathbf{r}}{\phi^{n^T}\mathbf{M}\phi^n} \tag{6-21}$$

These participation factors are determined by using the modal masses, M_1 and M_2, where

$$M_n = \phi^{n^T}\mathbf{M}\phi^n \tag{6-22}$$

Considering only terms to the order ε results in

$$L_1 = 1 - \gamma\varepsilon \tag{6-23}$$

and

$$L_2 = \gamma\varepsilon \tag{6-24}$$

The two participation factors define the effectiveness of the seismic isolation system. If the two system frequencies, ω_s and ω_b, are well separated, implying that $\omega_s >> \omega_b$, then L_2 is negligible and the corresponding structural deformation in the second mode is also negligible. The isolated structure is then effectively removed from the range of earthquake excitation when the frequency of the second mode shifts to a higher value than the frequency of the original non-isolated structure.

Furthermore, the negligibility of the second mode results in orthogonality with the seismic excitation. By the principle of orthogonality,

$$\phi^{n^T}\mathbf{M}\phi^1 = 0 \quad \text{for } n \neq 1$$

Given the assumption that

$$\mathbf{r} \approx \phi_1$$

seismic input is orthogonal to modes higher than the first, implying that

$$\phi^{n^T}\mathbf{M}\mathbf{r} \approx 0$$

This development results in the significant implication that the structure will be unaffected by the ground excitation even if the earthquake excitation frequency is in the same range as the frequency of the second mode. Thus, the seismic isolation deflects rather than absorbs input energy through orthogonality [18].

6.3 Damping and Energy Absorption

While seismic energy is essentially deflected by the isolation system to reduce absolute acceleration in the isolated mass, energy dissipation occurs locally within the isolators, reducing relative displacements. In the subsequent discussion, the effect of modal damping on the structure in terms of the modal damping factors will be determined. These factors are denoted as ξ^*_b for the isolator and ξ^*_s for the structure. The development assumes that elastometric isolation bearings are utilized, common in isolated bridge structures. It is also assumes that energy is dissipated through linear viscous damping. Similar to the preceding section, a more detailed discussion has been developed by Kelly [18].

In order to treat the modal damping factors separately, the equations of motion must remain uncoupled. To retain this decoupling, an approximate form of the damping factors, ξ^*_b and ξ^*_s, will be considered. The damping factor for the first mode, ξ^*_1, is synonymous with ξ^*_b, and the damping factor for the second mode, ξ^*_2, is synonymous with ξ^*_s. The approximation must be used because of the large difference in magnitude between the damping factors. Elastometric bearings are capable of exhibiting nearly 20% damping in the case of high damping natural rubber bearings, while the structure exhibits significantly less damping than the usually assumed value of 5% in earthquake analyses. This assumed value of 5% is based on hysteretic damping that occurs through earthquake damage resulting in plastic deformation in structural members. Since the seismic isolation system ideally protects the structure from inelastic deformations, a smaller damping value must be assumed.

To retain the decoupling of the equations of motion, the damping factors mentioned above, ξ^*_1 and ξ^*_2, are defined approximately as

$$2\omega_n^*\xi_n^* = \frac{\phi^{n^T}\mathbf{C}^*\phi^n}{\phi^{n^T}\mathbf{M}^*\phi^n} \tag{6-25}$$

Using the previously defined mode shapes and modal masses, it can be determined that

$$\xi_b^* = \xi_b\left(1-\frac{3}{2}\gamma\varepsilon\right) \tag{6-26}$$

and

$$\xi_s^* = \frac{\xi_s + \gamma\xi_b\sqrt{\varepsilon}}{\sqrt{(1-\gamma)}} \tag{6-27}$$

The above relationships show the significance of the damping in the elastometric bearing and its effect on the overall damping of the structure. Structural damping is increased to the order of $\varepsilon^{1/2}$, which can be significant considering that ξ_b is an order of magnitude greater than ξ_s. Thus, the high damping inherent in the rubber bearings contributes significantly to the overall energy dissipation in the structure, and displacements at the isolated level can be controlled primarily through damping in the isolation devices [18].

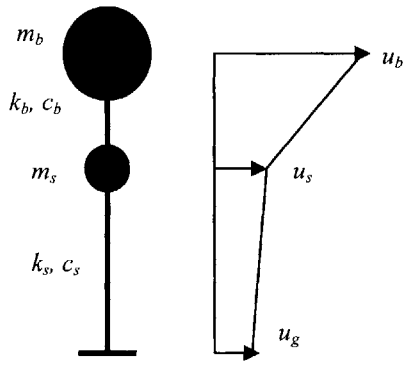

Figure 6-3: Refined two DOF model for bridge structure.

6.4 Simplified Application to Bridge Structures

The above discussion has been developed for the general case of seismic isolation, applicable to all structures, and illustrates the capability of isolation systems to deflect destructive earthquake energy. The phenomenon is essentially the same for

bridge structures, but the structural model differs slightly. In the case of bridge structures, isolation devices are generally located at the tops of supporting columns, isolating only the mass of the bridge superstructure. The refined model is shown above in Figure 6-3.

In this model, the isolated mass, m_b, represents the lumped mass of the deck superstructure. The isolator, having stiffness k_b and damping c_b, is located on top of the bridge pier. The stiffness and damping of the simplified pier structure are denoted by k_s and c_s respectively. The primary differences between the model shown above and the model discussed in Figure 6-1 are that the locations of the masses are inverted, and the isolated mass is large in comparison to the structural mass.

The equations of motion for this system are defined as follows

$$m_b\ddot{u}_b = -c_b(\dot{u}_b - \dot{u}_s) - k_b(u_b - u_s) \tag{6-28}$$

and

$$m_b\ddot{u}_b + m_s\ddot{u}_s = -c_s(\dot{u}_s - \dot{u}_g) - k_s(u_s - u_g) \tag{6-29}$$

Assuming that u_b is greater than u_s, the analysis is simplified by defining the relative displacements, v_b and v_b, as

$$v_b = u_b - u_s \tag{6-30}$$

and

$$v_s = u_s - u_g \tag{6-31}$$

The equations of motion then become

$$m_b\ddot{v}_b + m_b\ddot{v}_s + c_b\dot{v}_b + k_b v_b = -m_b\ddot{u}_g \tag{6-32}$$

and

$$(m_b + m_s)\ddot{v}_s + m_b\ddot{v}_b + c_s\dot{v}_s + k_s v_s = -(m_b + m_s)\ddot{u}_g \tag{6-33}$$

These equations can be rewritten in matrix form as

$$\begin{bmatrix} m_b + m_s & m_b \\ m_b & m_b \end{bmatrix} \begin{bmatrix} \ddot{v}_s \\ \ddot{v}_b \end{bmatrix} + \begin{bmatrix} c_s & 0 \\ 0 & c_b \end{bmatrix} \begin{bmatrix} \dot{v}_s \\ \dot{v}_b \end{bmatrix} + \begin{bmatrix} k_s & 0 \\ 0 & k_b \end{bmatrix} \begin{bmatrix} v_s \\ v_b \end{bmatrix} = -\begin{bmatrix} m_b + m_s & m_b \\ m_b & m_b \end{bmatrix} \begin{bmatrix} 1 \\ 0 \end{bmatrix} \begin{bmatrix} \ddot{u}_g \\ \ddot{u}_g \end{bmatrix} \quad (6\text{-}34)$$

As a rudimentary approximation, the above two DOF model can be approximated as a SDOF model, illustrated below in Figure 6-4 [13]. In this model, the mass of the isolated deck superstructure, m_s, and the mass of the bridge piers, m_b, are combined as one lumped mass at the top of the pier. K_{eq} denotes the combined equivalent lateral stiffness of the isolation devices and bridge piers, and C_{eq} denotes the combined damping contribution of the bridge piers and isolation devices.

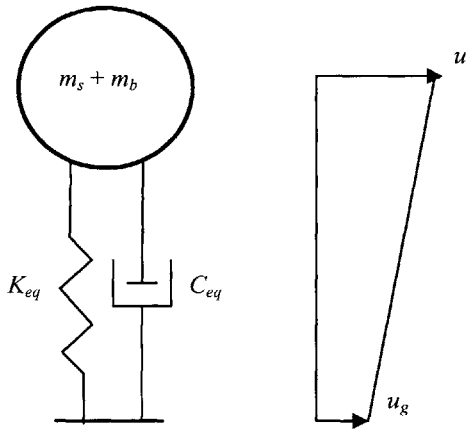

Figure 6-4: Simplified SDOF bridge model.

The equivalent lateral stiffness of the combined pier and isolator system for a single pier in terms of the isolator stiffness, k_b, and the pier stiffness, k_s, is denoted as

$$K_{eq} = \frac{\sum k_b}{1 + \frac{\sum k_b}{k_s}} \quad (6\text{-}35)$$

where

$\sum k_b$ = the combined stiffness of identical isolators located at a single pier.

If a bilinear elastometric isolation scheme is employed in the bridge structure, which is quite common in the seismic isolation of bridge structures, then the stiffness for a single isolator can be approximated as

$$k_b = \frac{F_{\max}}{u_{\max}} = \frac{F_y\left(1 - \frac{k_{pl}}{k_{el}}\right) + k_{pl}u_{\max}}{u_{\max}} \tag{6-36}$$

where k_{el} is the elastic stiffness of the isolation device, k_{pl} is the plastic stiffness of the isolation device, u_{max} is the maximum displacement of the isolator, and F_y is the yield strength of the hysteretic core of the isolator [13].

Because the model has been simplified to a single DOF system, the shifted period of the structure is dependent only upon the equivalent stiffness and combined deck and pier masses. The equivalent shifted period in the longitudinal direction of excitation, T_{eq}, is denoted by

$$T_{eq} = 2\pi\sqrt{\frac{\sum(m_s + m_b)}{\sum K_{eq}}} \tag{6-37}$$

The structural behavior discussed in this chapter is only an approximation of the mechanics of isolated structures and is used to illustrate the effectiveness of seismic isolation systems. A more accurate analysis is required in the actual design of isolation systems that incorporates three-dimensional geometries, the effects soil-structure interaction, and the effects of the transverse excitation of bridge structures.

CHAPTER 7: ANALYTICAL INVESTIGATION

7.1 Introduction

In order to gain a better understanding of the behavior of seismically isolated bridge structures, a comprehensive time history analysis was performed on a continuous multiple-span highway bridge using SAP2000 nonlinear finite element software [19]. The analyzed bridge was chosen as a representative example of typical simply supported highway bridges that often have fundamental periods in the range of the dominant excitation period of earthquakes and are consequently subjected to the greatest absolute acceleration and corresponding structural damage. The primary objectives of the study are to examine the effects of varying isolator stiffness on the relative displacement of the bridge superstructure at various joint locations, and to also observe the absolute accelerations and corresponding internal column shear forces in the different supporting columns.

7.2 Model Geometry

The dimensions of the model geometry were developed for reasons related to analytic accuracy. First, it was intended for the natural period of the bridge to correlate to the fundamental period of most simple span highway bridges of approximately 0.2 s to 1.2 s [14]. The calculated period of the non-isolated bridge is approximately 1.1 s, validating the accuracy of the model. Second, it was desired that the fundamental frequency of the structure be closely related to the dominant input seismic excitation frequency in order to exploit the seismic response of the structure. The results presented later in this section illustrate the achievement of this goal.

The model bridge consists of a 450 ft continuous span formed by three 150 ft segments supported by two piers of varying height. The piers have heights of 100 ft and 50 ft. The abutments are assumed to be infinitely stiff and thus do not contribute to the structural response. It is assumed that expansion joints are located at the abutments, and the superstructure is allowed to freely displace both laterally and longitudinally at the abutment locations. Pier footings were modeled using a fixed connection, assuming that the bridge is founded in bedrock and that the pier bases can neither translate in any

direction nor rotate about any axis. At the column-isolator interface, the column end joint is free to both translate and rotate. However, at the adjacent isolator-superstructure interface, the deck is restrained from translating in the vertical direction and can rotate only about the vertical axis. The conceptual geometry of the bridge is illustrated below in Figure 7-1, and the simplified model formulated for the SAP analysis is depicted in Figure 7-2.

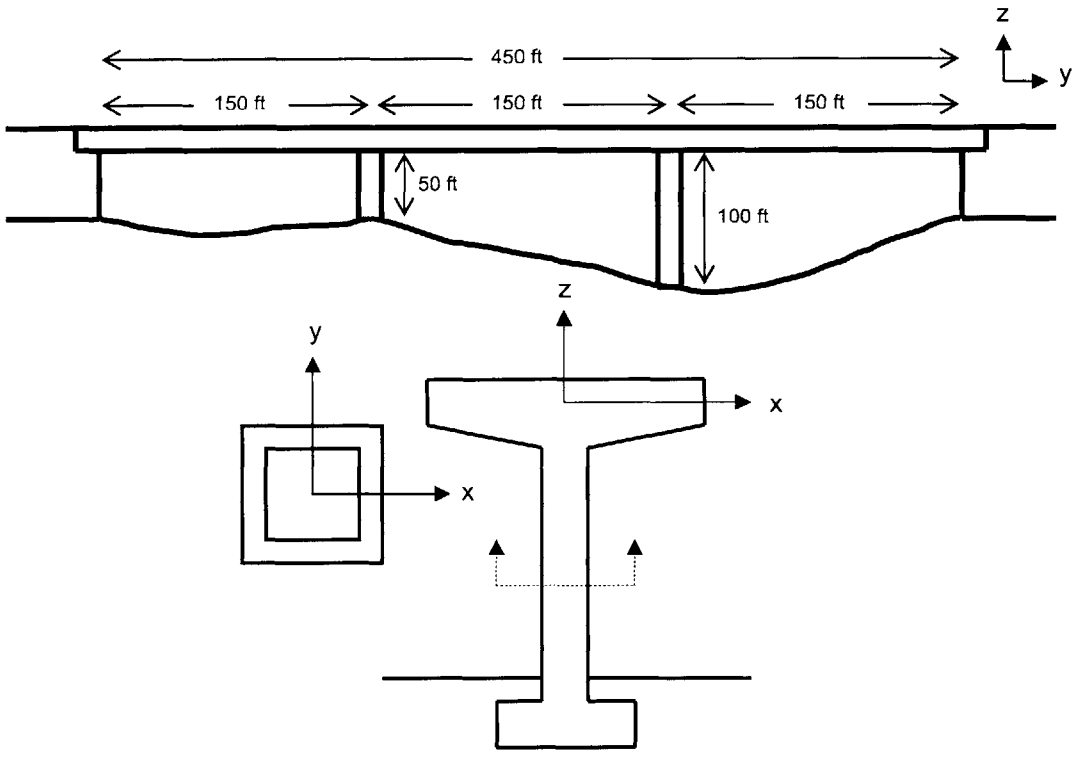

Figure 7-1: Conceptual geometry of analyzed model.

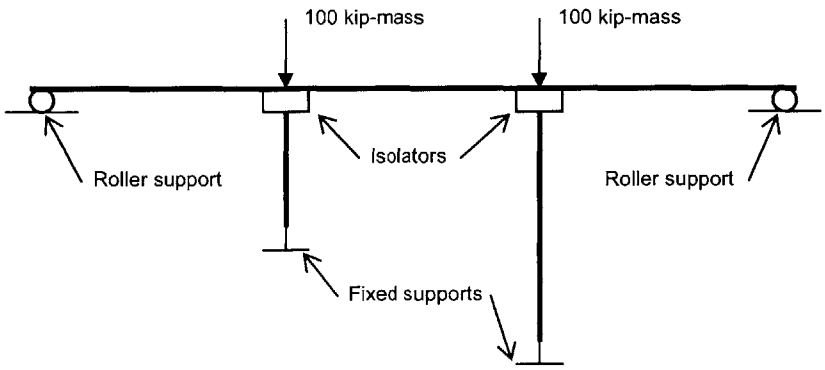

Figure 7-2: Simplified SAP2000 input geometry.

The two major structural components used in the bridge model are columns and deck sections. The geometric properties of these components, modified slightly to adhere to the assumed bridge geometry, are based upon an analysis performed by Priestly, et al. [1]. The geometric properties of the column and deck, namely cross-sectional area and area moment of inertia, are summarized below in Table 7-1 and Table 7-2, respectively.

Table 7-1: Column geometric cross-sectional properties.

Area (ft^2)	14.5
I_{xx} (ft^4)	865
I_{yy} (ft^4)	865
Weight (k/ft)	2.175

Table 7-2: Deck geometric cross-sectional properties.

Area (ft^2)	28
I_{zz} (ft^4)	10,221
I_{xx} (ft^4)	616
Weight (k/ft)	21.5

The linear weight of each component is also listed in the tables above. The linear weight of the deck section includes the dead load from the superstructure and the estimated live load due to traffic. This weight is lumped at the tops of the columns, illustrated in Figure 7-2, and used in the dynamic time history analysis. The value of the lumped mass at the top of each column is assumed to be 100 kip-mass, or 100,000 slugs. This mass is somewhat greater than that of a bridge of similar proportions, but the increased mass was utilized to obtain pronounced structural response to the applied excitation and to establish trends in the analysis.

7.3 Isolator Properties

The bridge bearings are modeled using bilinear hysteretic isolation bearings. The Nllink element in SAP2000, used to model local nonlinearities through effective linear and nonlinear properties, is utilized in the formulation of the bridge model. In particular, the Isolator1 element is used, which is recommended for the modeling of isolation devices. The element is adapted to bilinear hysteretic isolators that possess an elastic stiffness for linear analyses and an inelastic stiffness for nonlinear analyses [20].

As mentioned above, it is assumed that lead-rubber bearings are the isolation devices implemented in the bridge structure. One equivalent isolator is applied at the top of each column having the properties listed below in Table 7-3. The parameters listed in the table are depicted below in Figure 7-3 and Figure 7-4. In developing the model parameters, it is assumed that the diameter of the lead plug is 25% of the diameter of the entire isolation bearing and the maximum allowable shear strain in the elastometric material is 150%.

Table 7-3: Isolator properties used in nonlinear analysis.

H_{eff} (ft)	D_{iso} (ft)	D_{plug} (ft)	A_{plug} (in^2)	F_y (k)	u_y (ft)	k_{el} (k/ft)	k_{pl} (k/ft)	u_{max} (ft)	k_{eff} (k/ft)
0.250	0.50	0.125	1.8	3	0.0072	356	36	0.3750	42
0.500	1.00	0.250	7.1	10	0.0036	2,847	285	0.7500	297
0.625	1.25	0.313	11.0	16	0.0029	5,561	556	0.9375	571
0.750	1.50	0.375	15.9	23	0.0024	9,609	961	1.1250	979
1.000	2.00	0.500	28.3	41	0.0018	22,777	2,278	1.5000	2,302
1.250	2.50	0.625	44.2	64	0.0014	44,485	4,449	1.8750	4,479
1.375	2.75	0.688	53.5	78	0.0013	59,210	5,921	2.0625	5,955
1.500	3.00	0.750	63.6	92	0.0012	76,871	7,687	2.2500	7,724
1.625	3.25	0.813	74.7	108	0.0011	97,735	9,773	2.4375	9,813
1.750	3.50	0.875	86.6	126	0.0010	122,068	12,207	2.6250	12,250
2.000	4.00	1.000	113.1	164	0.0009	182,212	18,221	3.0000	18,270
2.250	4.50	1.125	143.1	208	0.0008	259,439	25,944	3.3750	25,999
2.500	5.00	1.250	176.7	256	0.0007	355,884	35,588	3.7500	35,650
3.000	6.00	1.500	254.5	369	0.0006	614,967	61,497	4.5000	61,570
3.500	7.00	1.750	346.4	502	0.0005	976,544	97,654	5.2500	97,741
4.000	8.00	2.000	452.4	656	0.0005	1,457,699	145,770	6.0000	145,868
4.500	9.00	2.250	572.6	830	0.0004	2,075,513	207,551	6.7500	207,662
5.000	10.00	2.500	706.9	1025	0.0004	2,847,068	284,707	7.5000	284,830
5.500	11.00	2.750	855.3	1240	0.0003	3,789,448	378,945	8.2500	379,080
6.000	12.00	3.000	1017.9	1476	0.0003	4,919,734	491,973	9.0000	492,121

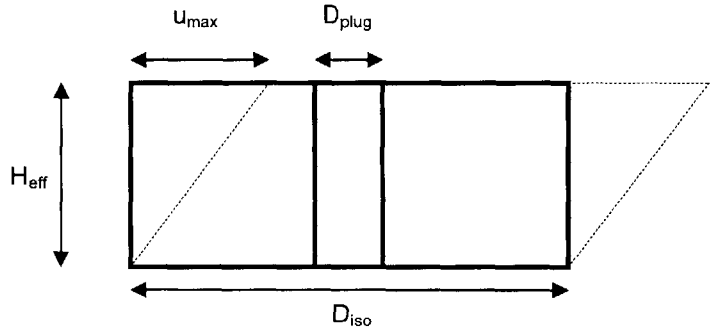

Figure 7-3: Parameters of isolator geometry.

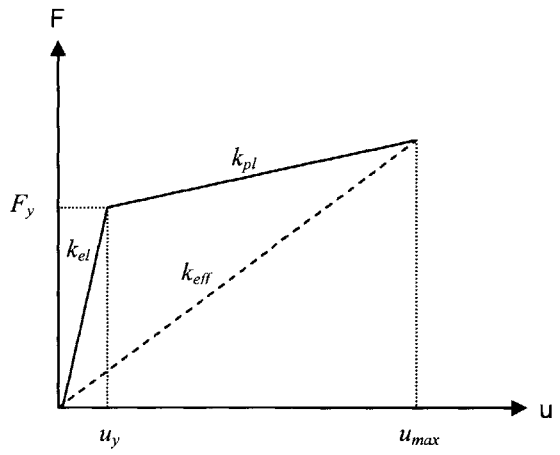

Figure 7-4: Parameters of isolator stiffness.

In the analysis of the model, it was assumed that the bearing properties at the top of each column are identical, even though the columns do not share the same geometry. Implementing bearings of identical stiffness for a bridge of unequal column heights would not be common in practice because the varying height and corresponding stiffness of each column group could induce a torsional response in the isolated bridge superstructure under transverse excitation. In general, isolation bearings are designed such that the center of mass of the structure coincides with the center of stiffness.

However, identical bearing properties at each column top were assumed for several reasons. First, the significance of equal bearing stiffness and the subsequent effects of the torsional response on the columns and relative joint displacements were desired. Second, isolation bearings of different stiffness designed to limit torsional effects from lateral excitation are generally designed assuming that ground motions are consistent at the footing of each supporting pier, which is not necessarily true [22]. Given the anisotropic and non-homogeneous nature of soil, the characteristics of seismic waves tend to change over the distance of propagation. This change can be particularly pronounced for bridge structures, where significant distances exist between supports and where geology and soil conditions are more apt to vary when the span crosses a water formation or irregular geologic formation. Thus, if consistent ground excitation at each support is assumed in the design of seismic isolation systems and actual ground excitation varies, then torsional vibration of the bridge superstructure may be induced.

This effect, however, is more problematic in long span bridges than in shorter simply supported bridge structures.

7.4 Earthquake Excitation

The north-south component of the 1940 El Centro earthquake in California, also known as the Imperial Valley earthquake, was chosen as the input excitation for the nonlinear time history analysis [22]. The earthquake magnitude measured 7.1 on the Richter Scale. The accelerogram for this earthquake is shown below in Figure 7-5. Spectral displacement, pseudo spectral velocity, and spectral acceleration graphs corresponding to 0%, 2%, and 5% of critical damping are illustrated in Figure 7-6, Figure 7-7, and Figure 7-8, respectively [11]. It is evident from these figures that the fundamental period of the modeled structure of 1.1 s lies in the range of the dominant excitation period of the El Centro earthquake.

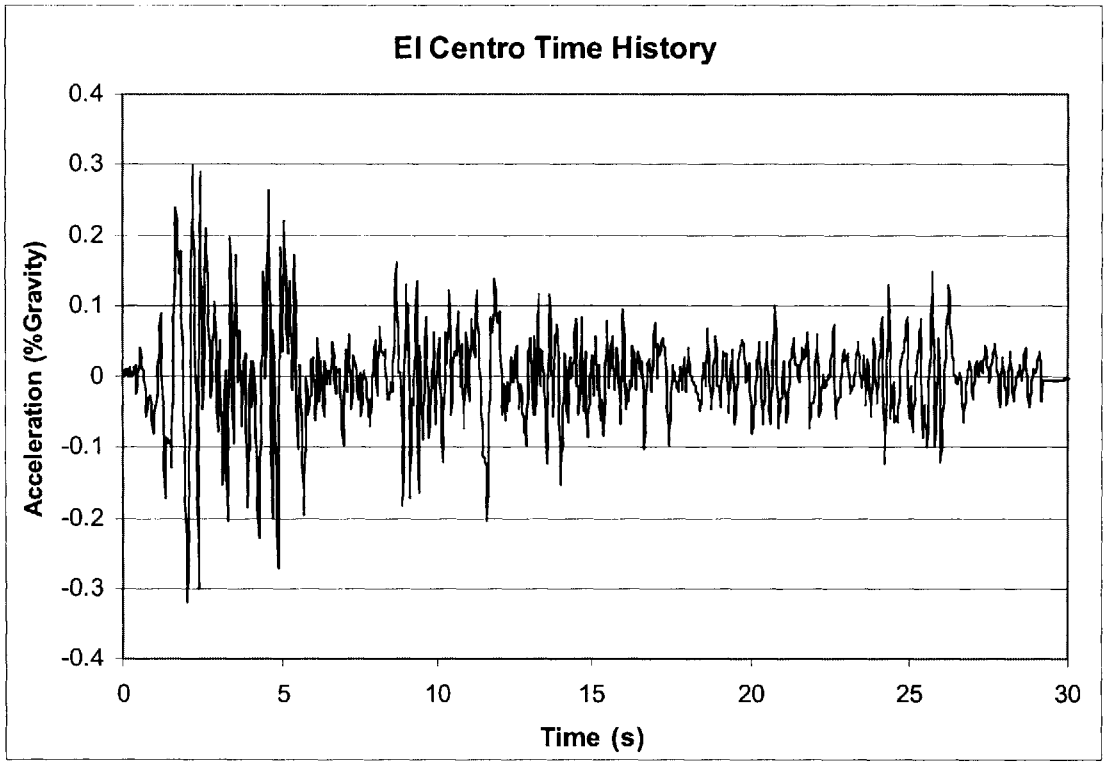

Figure 7-5: El Centro accelerogram.

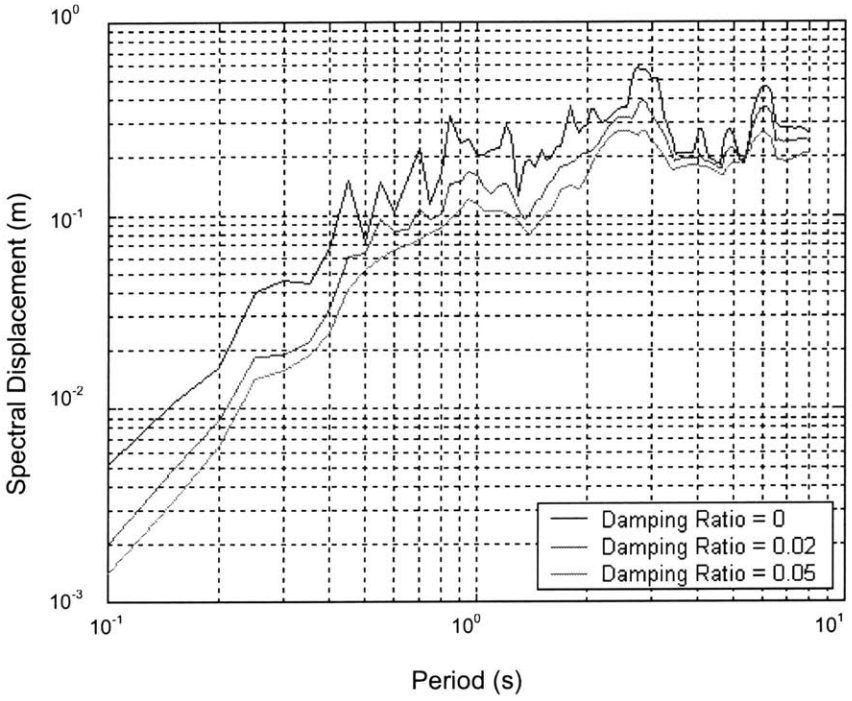

Figure 7-6: Spectral displacement – 1940 El Centro earthquake.

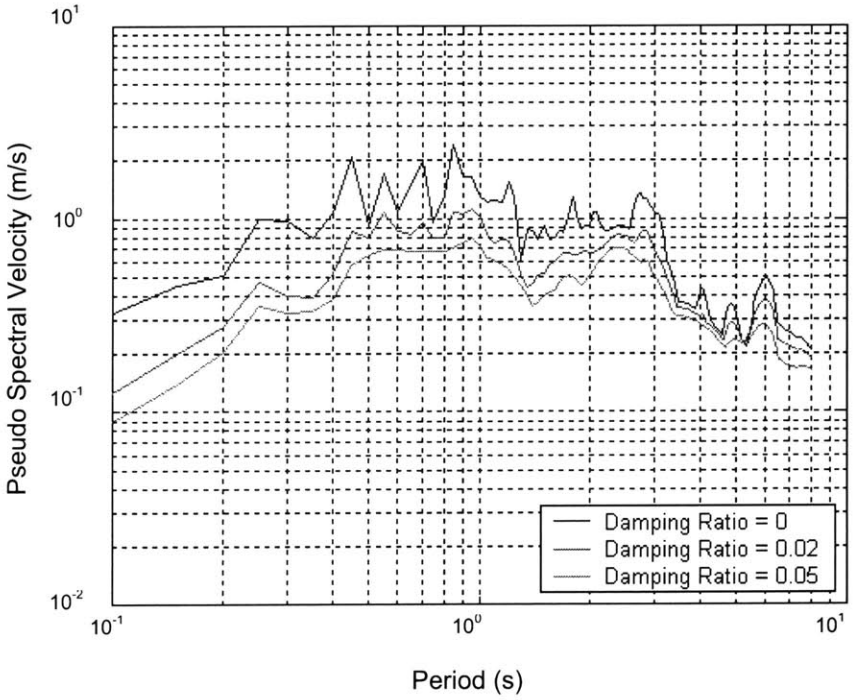

Figure 7-7: Pseudo spectral velocity – 1940 El Centro earthquake.

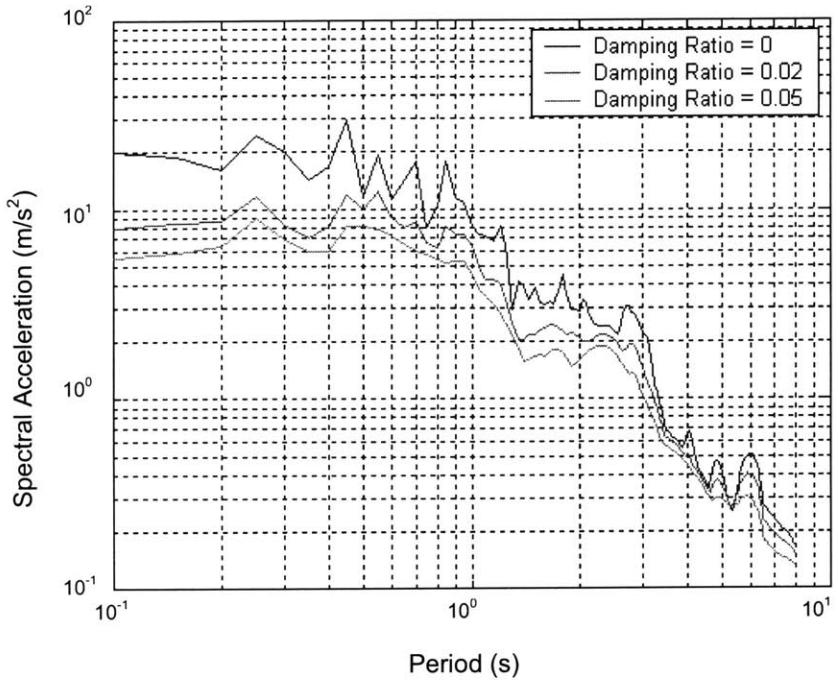

Figure 7-8: Spectral acceleration – 1940 El Centro earthquake.

7.5 Procedure

Multiple time-history analyses were performed to gage the effects of isolator stiffness upon the response of the structure. A trial was performed for each of the isolator properties listed in Table 7-3 using the same bridge geometry described above. The same earthquake excitation was applied to the bridge for each of the consecutive trials, and the earthquake excitation was applied in both the longitudinal and transverse directions. As a basis for comparison, an analysis was also performed for the same bridge structure without the application of isolation devices. Effective isolator stiffness was incrementally increased until the response of the structure mimicked that of the non-isolated structure. All relevant results are addressed later in this section.

7.6 Results

The aforementioned analyses were performed using SAP2000 finite element software, and the relevant findings are presented in the following discussion. The response of the structure to the earthquake excitation as dictated by the isolator properties is analyzed. This response includes the effects of isolator stiffness on fundamental period

shift, the maximum absolute acceleration induced in the supporting columns, and the maximum relative displacement of the superstructure. All graphs presented below include the stiffness ratio, represented as the normalized effective bearing height, $H_{eff}/H_{eff,max}$, on the abscissa, where $H_{eff,max}$ is taken as 6 ft. This is done for the sake of clarity convenience to illustrate trends that develop from increasing isolator stiffness. It should be reiterated that the effective height of the isolator used in this analysis represents the combined stiffness of multiple isolators located at the top of particular column group.

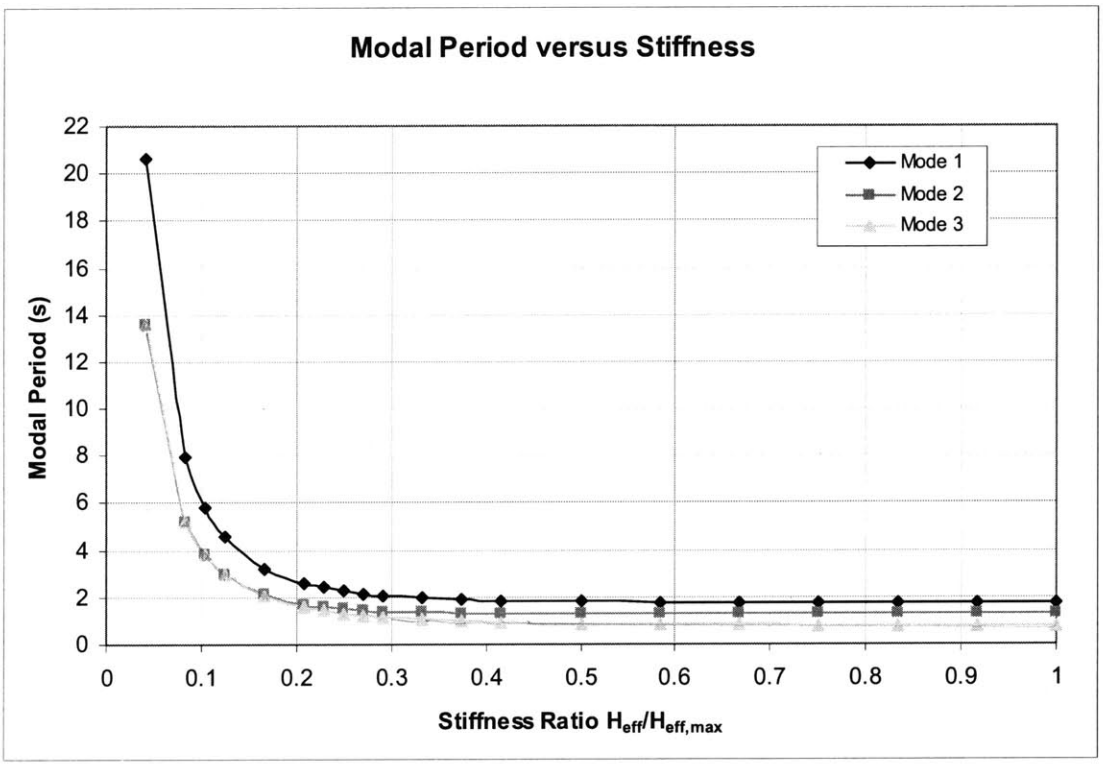

Figure 7-9: Modal period versus stiffness for isolated modes of vibration.

7.6.1 Period Shift

The effects of increasing isolator stiffness upon modal period are presented above in Figure 7-9. This figure shows the shifted periods of the first three modes of vibration of the bridge structure plotted against increasing values of effective isolator stiffness. Qualitative observations of the deflected mode shapes output by SAP2000 reveal that the

first three modes of vibration of the structure are the displacements of the isolated superstructure. The first mode is the torsional vibration of the bridge superstructure while the second and third modes of vibration are the lateral and longitudinal displacement of the isolated superstructure, respectively. It is evident in the figure that any stiffness increase beyond a fundamental period of approximately 2 s has a negligible effect on the period shift of the entire structure. It is also evident in the figure that the shifted period of the fundamental torsional mode remains consistently well-separated from the similar second and third modes as the effective stiffness of the isolators are increased. The implications of this separation will be discussed in a subsequent section.

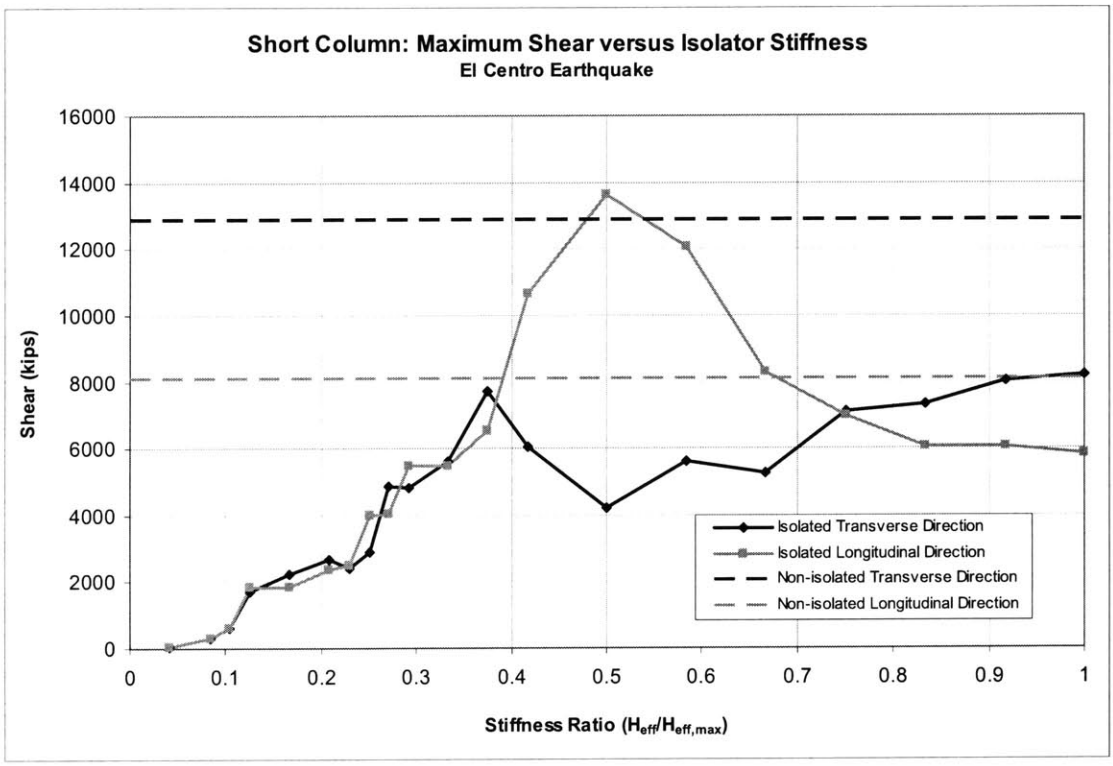

Figure 7-10: Maximum shear in short column.

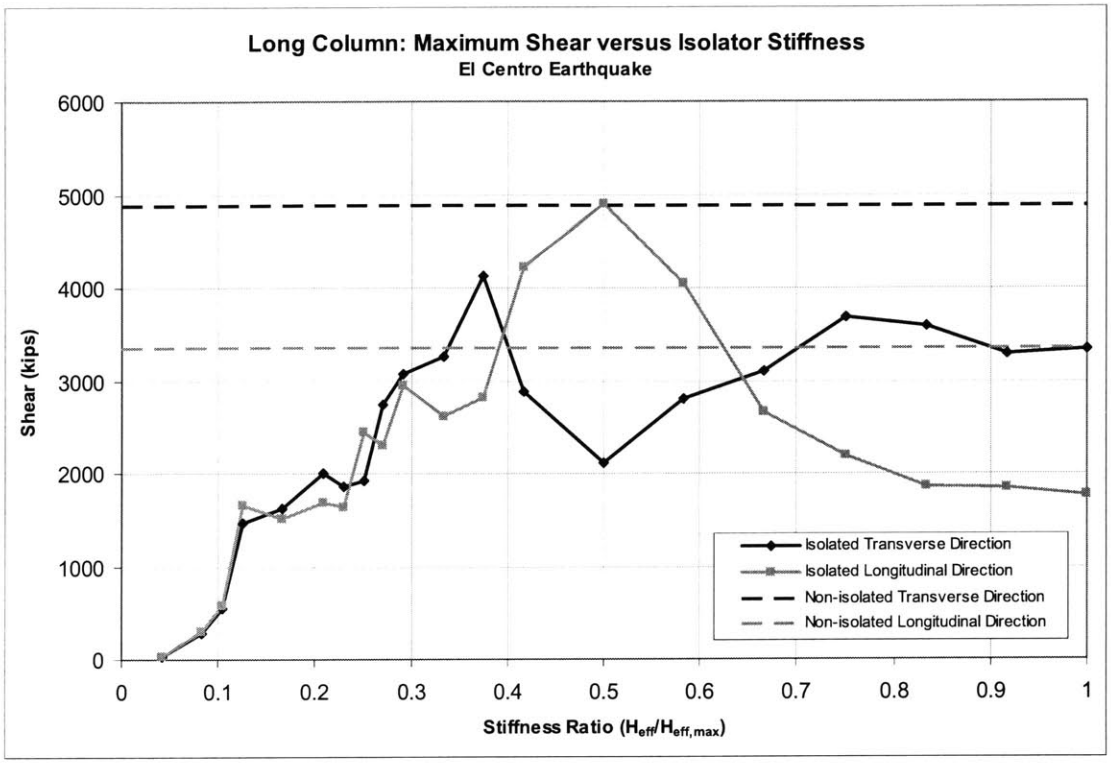

Figure 7-11: Maximum shear in long column.

7.6.2 Column Shear

The internal shear that develops in the supporting columns is an effect of the absolute acceleration experienced by the isolated superstructure. The maximum column shear that develops in the short and long columns in response to both the transverse and longitudinal directions of earthquake excitation are plotted above in Figure 7-10 and Figure 7-11, respectively. In the figures, the column shear is plotted as a function of the stiffness ratio of the isolator. The maximum shear experienced by the column for the complete earthquake time history for a particular isolator stiffness is plotted in each figure. Additionally, the maximum shear values of the non-isolated structures in the transverse and longitudinal directions are represented by the horizontal lines in the figures. Several notable characteristics within each figure can be observed, which will be discussed below.

First, it is evident from the general trend in shear values in both the short and long column that isolators having an equivalent effective stiffness ratio of less than

approximately 0.25, corresponding to a natural period of 2.25 s, are effective in isolating the structure from the damaging range of earthquake excitation. For isolators with implausible values of effective stiffness near zero, the corresponding column shear is also close to zero. As the effective stiffness of the isolators increases toward the maximum analyzed values, it can be seen that the values of column shear begin to approach shear values in the non-isolated structure, which is expected. This behavior is enforced by qualitative observations of the deformed shape of the model. As isolator stiffness was increased in the analysis, it was observed that the superstructure became progressively more coupled with the column substructure. With the increase in isolator stiffness, the first three deformation modes of the isolated superstructure were accompanied by significant deformation of the columns, indicating that the isolation system was no longer effective. This is evident in the column shear graphs in Figure 7-10 and Figure 7-11 and the modal period graph in Figure 7-9.

A second trend in the shear output reveals the achievement of resonance in the longitudinal direction at a stiffness ratio of 0.5, corresponding to a fundamental period of 1.8 s, in both the short and long columns. The value of shear at resonance in the longitudinal excitation direction the short column is much higher than in the long column due to the fact that the longer column is inherently less stiff and thus attracts smaller values of absolute acceleration. It can be accurately postulated that at the resonant stiffness ratio in the longitudinal direction, the structure is synchronized with a dominant excitation frequency of the earthquake and is not sufficiently isolated to appreciably reduce absolute acceleration. The structure's fundamental period of 1.8 s at which this behavior occurs corresponds to a local maximum in the spectral acceleration response spectrum of Figure 7-8. Thus, the structural response increases and shear values in the columns exceed even the values that are exhibited in the non-isolated structure.

Resonance in the longitudinal direction is accompanied by distinct local minima in the transverse direction of excitation for both columns. The occurrence of the local minima in the transverse direction raises several questions about the behavior of the structure. It can be postulated that the overall stiffness of the structure in a particular direction affects the response of the structure when subjected to excitation in a specified direction. However, in order to explain the achievement of a relative minimum value of

shear in the transverse direction as a simultaneous maximum value occurs in the longitudinal direction, it is necessary to conduct a more in depth analysis, such as examining the correlation between the maximum shear value and time of occurrence during the earthquake time history.

The achievement of shear values at resonance that are greater than shear values in the non-isolated structure emphasizes a crucial consideration in the design and implementation of isolated structures. The designer must pay careful attention to earthquake records in a specific location and must also consider the effects of local soil conditions upon wave propagation. It can be seen in the above graphs that even a small change in isolator stiffness can shift the fundamental frequency of the structure from a safely isolated range to directly within the dominant range of earthquake excitation. Thus, it is possible to increase structural damage in a deficiently designed seismic isolation system.

A final trend evident in the graphs is the occurrence of local maxima and minima in the range of effective stiffness just before resonance has been achieved. The possible causes of these local extremes can be explained by several suppositions. First, because the earthquake does not have a single specific dominant excitation frequency, it is possible that the bridge structure is being excited by frequencies outside the range of dominant excitation, which can be verified through a careful analysis of the acceleration response spectrum. Again, in order to more accurately explain this behavior, it is necessary to examine the time of occurrence of the extrema during the earthquake time history. A second possible cause is based upon the excitation of the higher isolated modes of the structure. In the analysis of seismic isolated structures, a single degree of freedom (SDOF) model is commonly used. In the SDOF model, only the first mode of vibration contributes to the structural response, which is the vibration of the isolated portion of the structure. In the bridge model used in this analysis, however, the geometry and structural stiffness result in the first three modes of vibration characterized by the deformation of the isolated structure. As mentioned above, the first mode of vibration is the torsional mode, which is well-separated from the second and third modes of longitudinal and transverse vibration. Thus, the possibility exists that the structure is excited by earthquake excitation periods that correspond to the periods of the second and

third isolated modes of vibration, resulting in local maxima and minima in column shear as isolator stiffness is gradually increased. Again, to verify this explanation, a more detailed analysis must be conducted.

7.6.3 Relative Joint Displacements

A second consequence of seismic isolation, relative joint displacement, is also examined in the analysis of the bridge model. In this discussion, the relative displacement of the superstructure in both the longitudinal and transverse directions with respect to the column base at observation points located immediately above the two supporting columns is studied as a function of isolator stiffness. In addition, the relative displacement between the superstructure and the column tops is examined, which is synonymous with the shear deformation of the isolators at the top of each column.

7.6.3.1 Superstructure Displacement Relative to Column Base

The maximum relative displacements of the superstructure during the entire earthquake time history for a particular isolator stiffness in both the longitudinal and transverse directions of excitation at two specified locations are plotted below in Figure 7-12 and Figure 7-13. Figure 7-12 illustrates the relative displacement of the deck superstructure at a location immediately above the shorter column while Figure 7-13 illustrates the relative displacement of the deck superstructure at a location immediately above the longer column. The maximum superstructure displacement of the non-isolated structure at the two aforementioned locations is also plotted in the graphs.

Several trends can be observed in the examination of the relative displacements of the deck shown in Figure 7-12 and Figure 7-13. The first trend exhibits the effectiveness and expected behavior of the isolated structure. For a highly flexible isolation system, the initial displacement is relatively significant and as isolator stiffness increases, the joint displacements approach the relative displacement values of the non-isolated structure. As the isolators become stiffer, the superstructure becomes increasingly coupled with the substructure, and the relative displacement of the isolated superstructure approaches the relative displacement of the non-isolated superstructure. The relative displacement behavior of the deck at the locations of the two column tops is nearly

identical in magnitude for the isolated structure. The relative displacement of the deck of the non-isolated structure is expectedly greater atop the more flexible long column than atop the short column.

A second noticeable trend is the abrupt development of maximum relative displacement corresponding to a stiffness ratio of 0.125. For an isolated structure, it is generally expected that relative displacement of the isolated superstructure will be greatest for lower isolator stiffness and will subsequently decrease for higher isolator stiffness values. The seemingly anomalous peak displacement, however, can be explained in terms of isolator properties and earthquake spectral displacement. If the spectral displacement graph of Figure 7-6 is examined, then it can be observed that local maxima occur at structural periods of approximately 5 s and 6 s. The effective stiffness values of the isolated bridge structure that relate to the resonant range exhibited in Figure 7-12 and Figure 7-13 have corresponding periods in the range of 5 s to 6 s, thus explaining the peaks in the graphs. This behavior would likely be more discernable with a more in depth analysis where the effective stiffness of the isolator is selected such that the resulting structural period corresponds to peak periods in the spectral displacement plot. It can be noticed in the spectral displacement plot, however, that even greater spectral displacements exist at lower periods. When the structure possesses these periods, the isolators are significantly stiffer, and the superstructure is more coupled with the substructure. Thus, significant relative displacements are no longer achieved.

The third noteworthy trend involves the above discussion concerning the internal shear behavior in the columns. A local maximum for displacement in the longitudinal direction and a local minimum for displacement in the transverse direction can be observed at a stiffness ratio of approximately 0.5, which corresponds to the well-defined maxima and minima in the shear versus stiffness graphs in Figure 7-10 and Figure 7-11. Possible reasons for this behavior were addressed in the previous section. Other local maxima and minima are also evident in the figures. Postulated reasons for this behavior, such as the excitation of higher isolated modes and response to varying excitation frequencies, are also addressed in the above explanation of column shear behavior. Ultimately, a more detailed analysis is required to accurately explain this behavior.

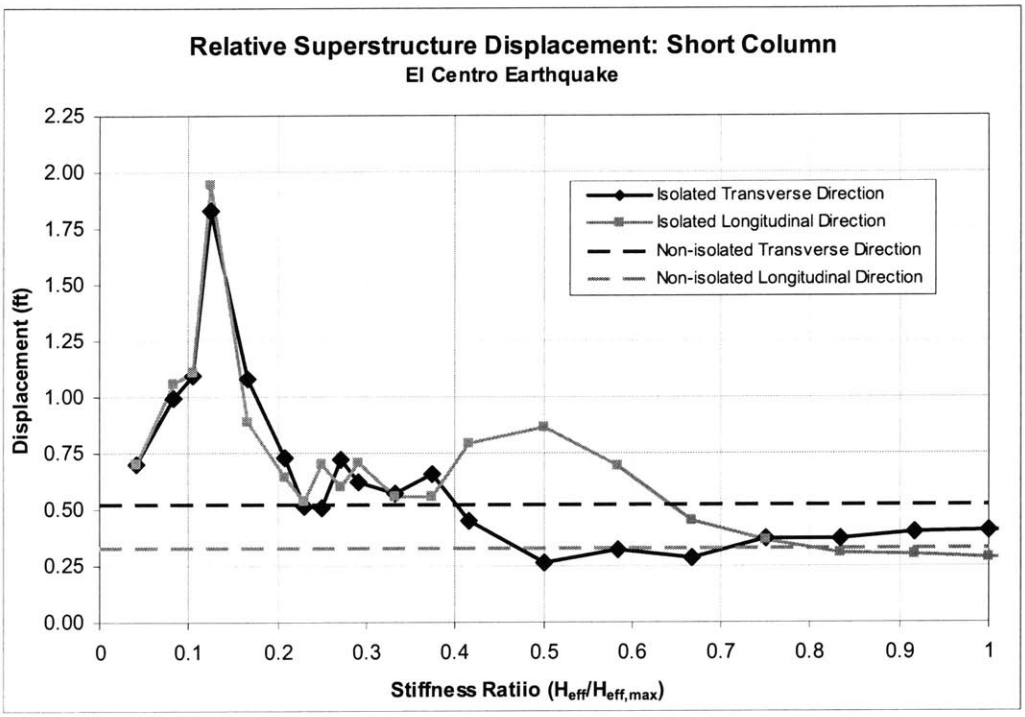

Figure 7-12: Longitudinal and transverse relative displacement of the superstructure above the short column.

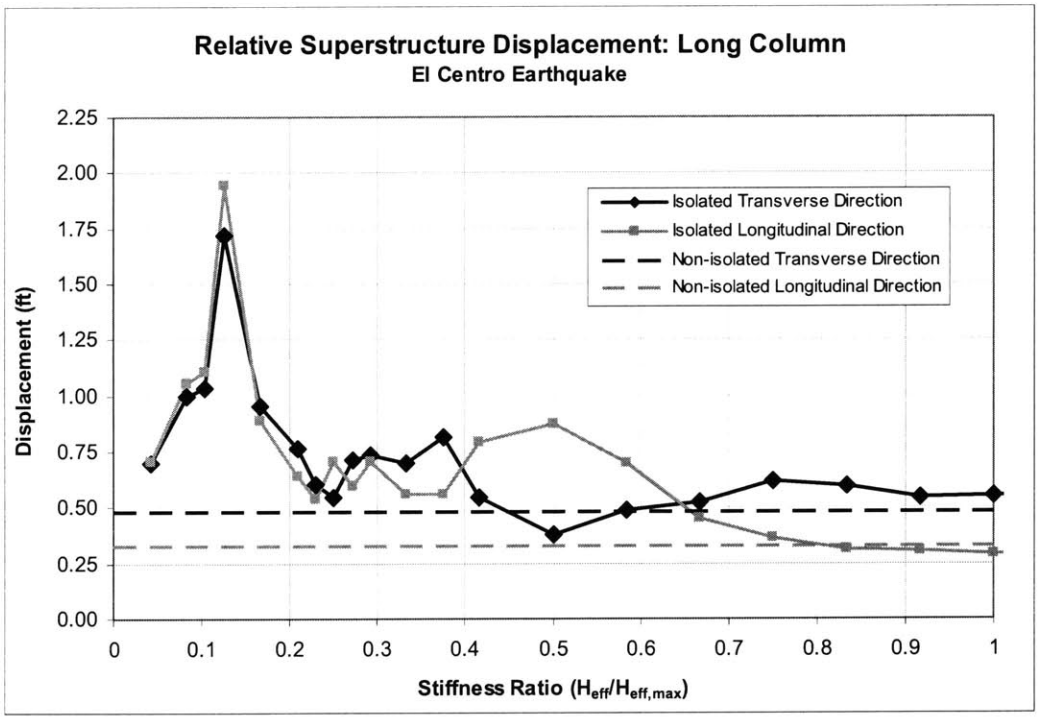

Figure 7-13: Longitudinal and transverse relative displacement of the superstructure above the long column.

7.6.3.2 Isolator Shear Deformation

The relative displacement between the superstructure and column tops, which represents the shear deformation of the isolators, is plotted below in Figure 7-14 through Figure 7-17. Figure 7-14 illustrates the shear deformation of the isolator at the top of the short column in the transverse direction, and Figure 7-15 illustrates the same relationship in the longitudinal direction. Similarly, Figure 7-16 shows the isolator shear deformation at the top of the long column in the transverse direction, while Figure 7-17 depicts the same relationship in the longitudinal direction.

In general, the relative displacement relationship between the stated components is similar. As expected, the difference between the displacement of the superstructure and substructure decreases as the isolator stiffness increases. Eventually, the shear deformation between components becomes negligible, at which point the superstructure is fully coupled with the substructure. Additionally, the displacement behavior regarding the existence of local maxima and minima addressed in the previous section is evident in each of the below figures.

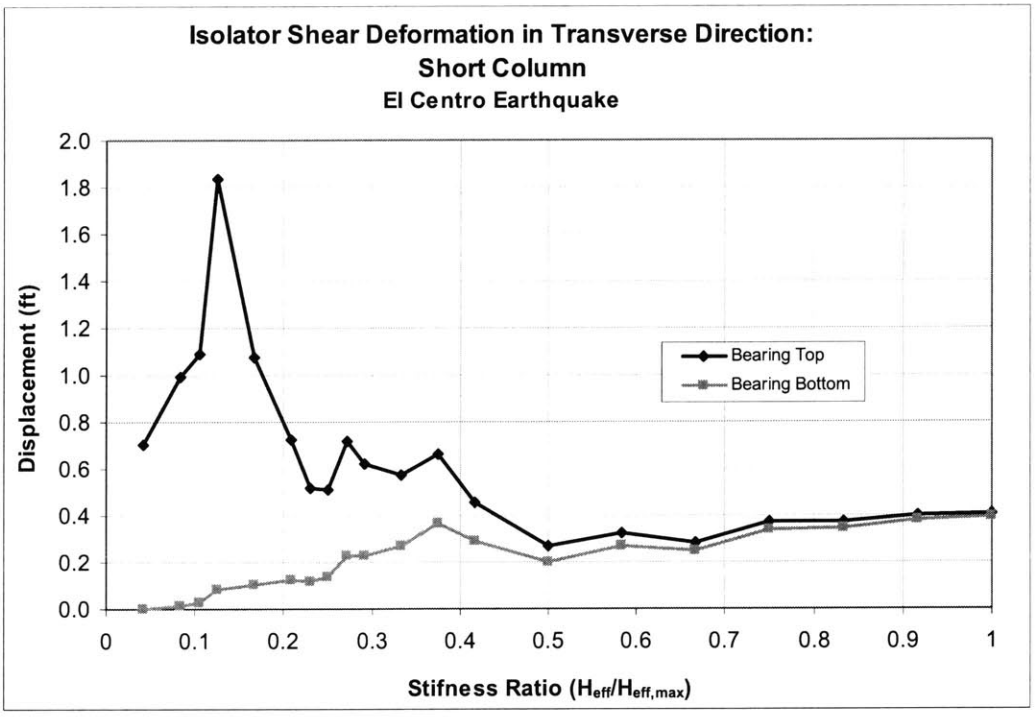

Figure 7-14: Relative joint displacement at top of short column – transverse excitation direction.

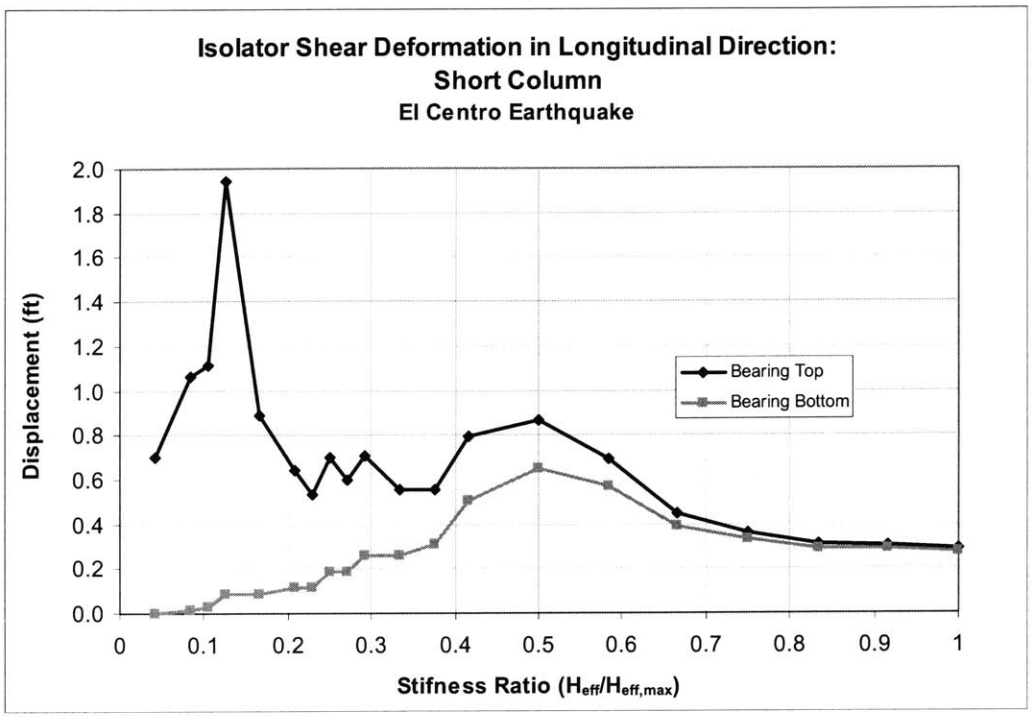

Figure 7-15: Relative joint displacement at top of short column – longitudinal excitation direction.

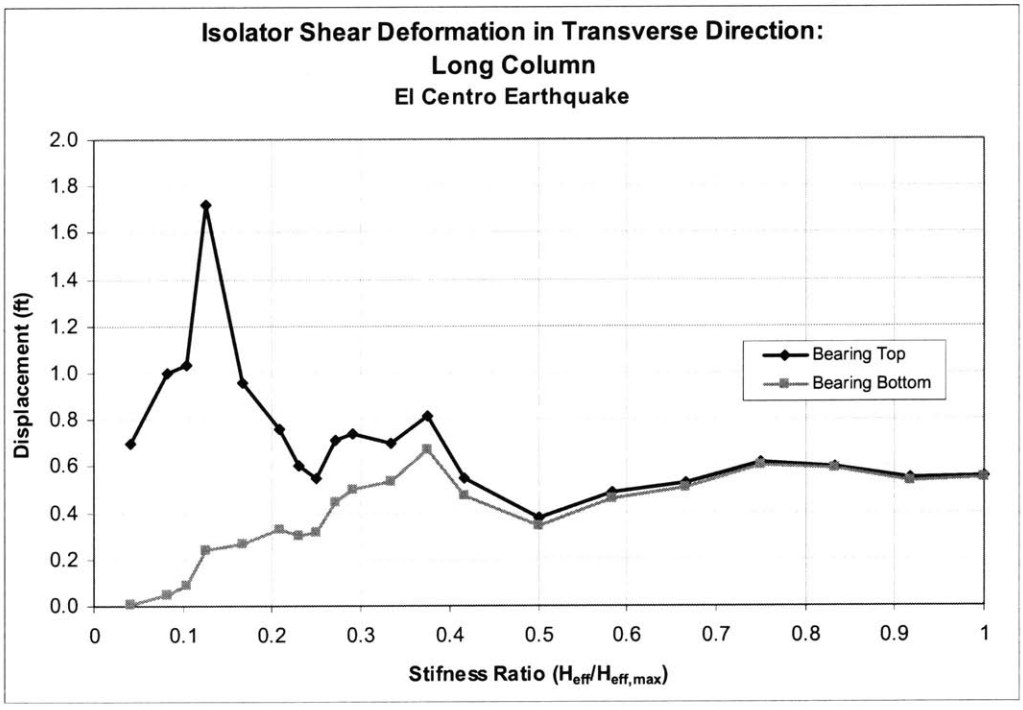

Figure 7-16: Relative joint displacement at top of long column – transverse excitation direction.

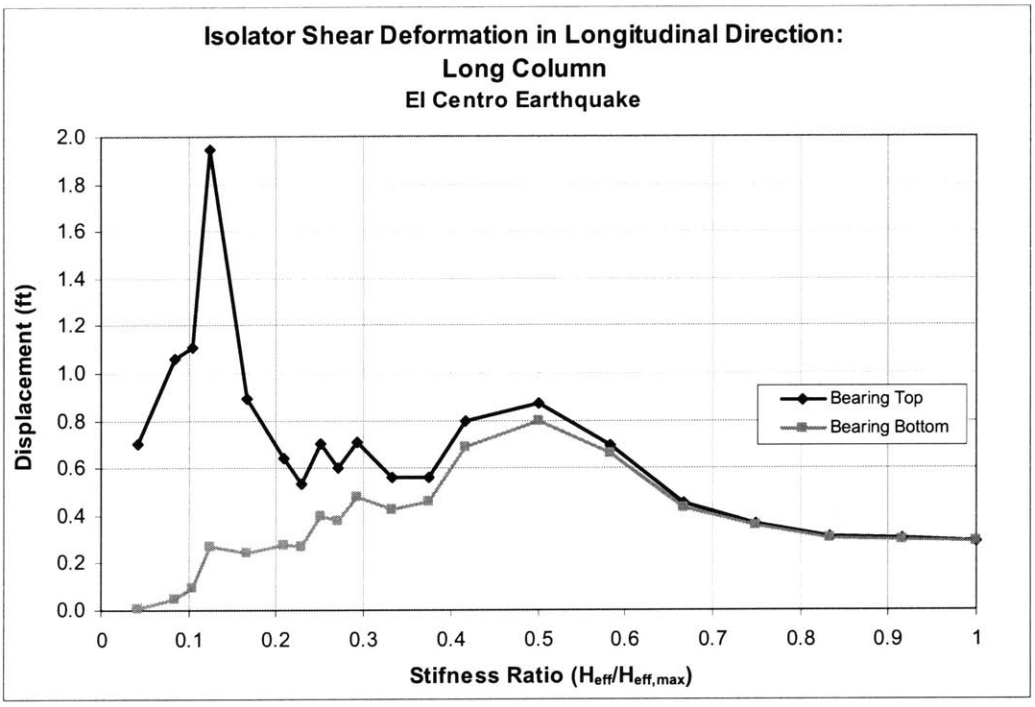

Figure 7-17: Relative joint displacement at top of long column – longitudinal excitation direction

CHAPTER 8: CONCLUSION

It was stated by Dr. Charles F. Richter that "Only fools, charlatans, and liars predict earthquakes" [23]. Given the unpredictable nature of seismic events, society must safely and effectively protect public infrastructure from earthquake damage to prevent destruction and loss of life. Bridges warrant special attention in earthquake resistant design as they are a primary component of the industrialized world's highway system and are particularly vulnerable to earthquake damage. Seismic isolation has proven to be both an attractive and effective means to reduce destructive seismic forces in bridge structures, and the technology continues to gain popularity in both the retrofit of existing structures and the design of new structures.

The effectiveness of seismic isolation is particularly noticeable when compared to failures resulting from bridges designed using an elastic design philosophy and even bridges that were retrofitted with non-isolation strategies. Earthquakes that have occurred within the past decade have caused significant damage to many of these bridges, emphasizing the need for a more effective method to resist seismic forces. Major damage has occurred to the supporting columns of simple span bridges as columns lack the capacity to resist increased shear and flexure induced during seismic excitation.

Induced forces within the supporting bridge columns can be avoided through the implementation of seismic isolation systems. These isolation systems effectively decouple the deck superstructure from the supporting column substructure, lengthening the fundamental period of the structure. The shifted period removes the structure from the range of dominant earthquake excitation, and absolute acceleration experienced by the structure is consequently reduced.

The behavior of seismic isolation systems applied to bridge structures has been investigated through a non-linear time history analysis conducted using a continuous span bridge and elastometric lead-rubber isolation bearings. The effect of isolator stiffness on column shear and superstructure displacement was examined in response to the 1940 El Centro earthquake, and results are consistent with the expected behavior of isolated structures.

While seismic isolation is clearly an effective means to reduce destructive seismic forces in structures, it should be reiterated that sufficient care must be taken in the design of isolation systems to avoid shifting the structural period into the dominant range of earthquake excitation, as demonstrated in the analytical investigation. In order to achieve the most efficient isolation system design, earthquake time histories for the specific site and orientation of a structure must be examined in addition to the effects of soil conditions on seismic wave propagation at the site.

Seismic isolation systems are a remarkable and well-established innovation that has saved countless lives and public dollars. Their future implementation in developing countries, in addition to their effectiveness and structural applicability, ultimately lies with the education and resolve of the engineer.

CHAPTER 9: REFERENCES

[1] M. J. N. Priestley, F. Seible, and G. M. Calvi, *Seismic Design and Retrofit of Bridges*. New York: John Wiley, 1996.

[2] James D. Cooper, Ian M. Friedland, Ian G. Buckle, Roland M. Nimis, and Nancy McMullin Bobb, "The Northridge Earthquake: Progree Made, Lessons Learned in Seismic-Resistant Bridge Design," *FHWA Public Roads Online*, vol 58, no. 1, Mar. 2004; <http://www.tfhrc.gov/pubrds/summer94/p94su26.htm>.

[3] Farzad Naeim and James M. Kelly, *Design of Isolated Structures from Theory to Practice*. New York: John Wiley & Sons, 1999.

[4] United States Geological Survey (USGS), "When Could the Next Large Earthquake Occur Along the San Andreas Fault?" Mar. 2004; <http://pubs.usgs.gov/gip/earthq3/when.html>.

[5] University of Calgary, "Structural & Geotechnical Engineering," Mar. 2004; <http://www.eng.ucalgary.ca/CSCE-Students/structural_earthquakes.htm>.

[6] Kenneth M. Leet and Dionisio Bernal, *Reinforced Concrete Design*. Boston: McGraw-Hill, 1997.

[7] Hamid Ghasemi, "Seismic Protection of Bridges," *FHWA Public Roads Online*, vol. 62, no. 5, Mar. 2004; <http://www.tfhrc.gov/pubrds/marapr99/seismic.htm>.

[8] Oral Büyüköztürk, class notes for 1.541, Department of Civil and Environmental Engineering, Massachusetts Institute of Technology, Spring 2004.

[9] ACE-MRL, "Earthquake Hazard Mitigation," Mar. 2004; <http://acemrl.engin.umich.edu/NewFiles/projects/seis_overview.html>.

[10] Eduardo Kausel, and José Manuel Roësset, *Advanced Structural Dynamics*. Unpublished, Massachusetts Institute of Technology, 2001.

[11] Jerome J. Connor and Stefan F. D'Heedene, *SPECTRA*. Computer software, Unpublished, Massachusetts Institute of Technology, 2001.

[12] Ian G. Buckle, Ronald L. Mayes, and Martin R. Button, *Seismic Design and Retrofit Manual for Highway Bridge FHWA-IP-87-6*. McLean, Virginia: Federal Highway Administration, 1987.

[13] P. Komodromos, *Seismic Isolation for Earthquake Resistant Structures*. Southhampton: WIT Press, 2000.

[14] M. C. Kunde and R. S. Jangid, "Seismic Behavior of Isolated Bridges: A State-of-the-Art Review," *Electronic Journal of Structural Engineering*, vol. 3, pp. 140-170, 2003.

[15] Eugene Ehrlich, Stuart Berg Flexner, Gorton Carruth, and Joyce M. Hawkins. *Oxford American Dictionary*, New York: Avon Books, 1980.

[16] Jerome J. Connor, *Introduction to Structural Motion Control*, Upper Saddle River: Prentice Hall, 2003.

[17] M. Fragiacomo, S. Rajgelj and F. Cimadom, "Design of Bilinear Hysteretic Isolation Systems," *Earthquake Engineering and Structural Dynamics*, vol. 32, pp. 1333-1352, 2003.

[18] James M Kelly, *Earthquake-Resistant Design with Rubber*. London: Springer Verlag, 1997.

[19] Computers and Structures, Inc, *SAP2000*. Computer Software. Computers and Structures, Inc., 1998.

[20] Computers and Structures, Inc., *SAP2000 Analysis Reference*. Computers and Structures, Inc., 1998.

[21] Giovanna Zanardo, Hong Hao, and Claudio Modena, "Seismic Response of Multi-Span Simply Supported Bridges to a Spatially Varying Earthquake Ground Motion." *Earthquake Engineering and Structural Dynamics*, vol. 31, 1325-1345, 2002.

[22] Tom Irvine, "El Centro Earthquake," Apr. 2004; <http://www.vibrationdata.com/elcentro.htm>.

[23] Per Bak, *How Nature Works: The Science of Self-Organized Criticality*, New York: Copernicus, 1996.